

Radiative Production of Lightest Neutralinos in e^+e^- collisions in Supersymmetric Grand Unified Models

P. N. Pandita,¹ Monalisa Patra²

¹ *Department of Physics, North Eastern Hill University, Shillong 793 002, India*

² *Centre for High Energy Physics, Indian Institute of Science, Bangalore 560 012, India*

We study the production of the lightest neutralinos in the radiative process $e^+e^- \rightarrow \tilde{\chi}_1^0 \tilde{\chi}_1^0 \gamma$ in supersymmetric models with grand unification. We consider models wherein the standard model gauge group $SU(3)_c \times SU(2)_L \times U(1)_Y$ is unified into the grand unified gauge groups $SU(5)$, or $SO(10)$. We study this process at energies that may be accessible at a future International Linear Collider. We compare and contrast the dependence of the signal cross section on the grand unified gauge group, and different representations of the grand unified gauge group, into which the standard model gauge group is unified. We carry out a comprehensive study of the radiative production process which includes higher order QED corrections in our calculations. In addition we carry out a detailed study of the background to the signal process coming from the Standard Model radiative neutrino production $e^+e^- \rightarrow \nu \bar{\nu} \gamma$, as well as from the radiative production of the scalar partners of the neutrinos (sneutrinos) $e^+e^- \rightarrow \tilde{\nu} \tilde{\nu}^* \gamma$. The latter can be a major supersymmetric background to the radiative production of neutralinos when the sneutrinos decay invisibly. It is likely that the radiative production of the lightest neutralinos may be a viable channel to study supersymmetric partners of the Standard Model particles at the first stage of a International Linear Collider, where heavier sparticles may be too heavy to be produced in pairs.

PACS numbers: 11.30.Pb, 12.60.Jv, 14.80.Ly

I. INTRODUCTION

Supersymmetry (SUSY) [1] is a leading candidate for physics beyond the standard model (SM). In supersymmetric models the Higgs sector of the SM is technically natural [2]. Since supersymmetry is not an exact symmetry in nature, it must be broken in realistic models of supersymmetry. Although the precise manner in which SUSY is broken is not known at present, in actual practice necessary SUSY breaking can be introduced through soft supersymmetry breaking terms that do not reintroduce quadratic divergences in the Higgs mass, and thereby do not disturb the stability of the hierarchy between the weak scale and a large scale (grand unified (GUT), or Planck scale). The simplest implementation of the idea of softly broken supersymmetry is the Minimal Supersymmetric Standard Model (MSSM) obtained by introducing the supersymmetric partners of the SM states, and introducing an additional Higgs doublet, with opposite hypercharge to that of the SM Higgs doublet, in order to cancel the gauge anomalies and generate masses for all the fermions of the Standard Model [3]. If we want broken supersymmetry to be effective in protecting the Higgs mass against large radiative corrections, then the supersymmetric partners of the Standard Model (SM) particles cannot be much heavier than about 1 TeV. The discovery of the superpartners of the SM particles is one of the main goals of present and future accelerators.

When the SM gauge symmetry $SU(2) \times U(1)$ is broken, the fermionic partners of the two Higgs doublets (H_1, H_2) of the MSSM mix with the fermionic partners of the gauge bosons, resulting in four neutralino states $\tilde{\chi}_i^0$, $i = 1, 2, 3, 4$, and two chargino states $\tilde{\chi}_j^\pm$, $j = 1, 2$. In several models of low energy supersymmetry, the lightest neutralino is typically the lightest supersymmetric particle (LSP). In the MSSM, if we assume R -parity (R_p) conservation, then the lightest supersymmetric particle is absolutely stable. There has been extensive study of the neutralino states of the minimal supersymmetric standard model, and its extensions [4–12], because the lightest neutralino, being the LSP, is the end product of any process that involves supersymmetric particles in the final state. In this work we will assume that the LSP is the lightest neutralino, it is stable, and that it escapes the collider experiments undetected. The composition and mass of the neutralinos and charginos will play a key role in the search for supersymmetry at high energy accelerators. The composition and mass of neutralinos will also determine the time-scale of their decays. The implications of mass patterns of the neutralinos in models with different particle content, or with specific SUSY breaking patterns were considered in some detail in [8, 11, 12].

At present an indirect phenomenological evidence for supersymmetry is obtained from the unification of the gauge couplings of the Standard Model in supersymmetric grand unified theories (GUTS) [13, 14]. Furthermore, one of the most important prediction of grand unification is that of baryon number violating interactions, leading to proton decay. However, in supersymmetric grand unified theories proton decay is much slower than in nonsupersymmetric grand unified theories. The reason for this is that the unification scale in supersymmetric

GUTS is of the order of $M_{\text{GUTS}} \sim \text{few} 10^{16}$ GeV, which is about 20 – 30 times larger than the corresponding scale in non-SUSY GUTS. Thus, proton decay via gauge boson exchange is negligible and main decay arises from dimension-5 operators with higgsino exchange. This leads to a rate of proton decay which is close to the existing bounds [15]. Furthermore, the range of neutrino masses as indicated by current experiments, when interpreted in terms of see-saw mechanism, point towards a large scale consistent with the scale M_{GUTS} of supersymmetric grand unification [16].

It is, thus, natural to study the phenomenology of neutralino and charginos in an underlying grand unified theory. Most of the studies involving neutralinos and charginos in the minimal supersymmetric standard model have been performed with universal gaugino masses at the grand unification scale [17]. The neutralino and chargino masses depend on the soft $SU(2)_L$ and $U(1)_Y$ gaugino masses M_2 and M_1 , the higgs(ino) parameter μ , and $\tan\beta \equiv v_2/v_1$, where v_2 and v_1 are the vacuum expectation values of the neutral components of the two Higgs doublets H_2 and H_1 . Most of the models assume the gaugino mass universality at the GUT scale, i.e. $M_1 = M_2 = M_3$, where M_3 is the $SU(3)_C$ soft gaugino mass. However, there is no specific theoretical reason for the choice of universal masses at the grand unification scale. It is possible to have nonuniversal gaugino masses in grand unified theories wherein the standard model gauge group is embedded in a grand unified gauge group. In a given supersymmetric model gaugino masses are generated from higher dimensional interaction terms involving gauginos and auxiliary parts of chiral superfields [18]. As an example, in $SU(5)$ grand unified theory (GUT), the auxiliary part of a chiral superfield in higher dimensional terms can be in the representation **1**, **24**, **75**, or **200**, or, in general, some combination of these representations. When the auxiliary field of one of the $SU(5)$ nonsinglet chiral superfields obtains a vacuum expectation value (VEV), then the resulting gaugino masses are nonuniversal at the grand unification scale. Similar conclusions hold for other supersymmetric grand unified models. Furthermore, nonuniversal supersymmetry breaking masses are a generic feature in some of the realistic supersymmetric models. For example, in anomaly mediated supersymmetry breaking models the gaugino masses are not unified [19, 20], and hence are not universal.

From above discussion it is clear, that the phenomenology of supersymmetric models depends crucially on the composition of neutralinos and charginos. This in turn depends on the soft gaugino mass parameters M_2 and M_1 , besides the parameters μ and $\tan\beta$. Since most of the models discussed in the literature assume gaugino mass universality at the GUT scale, it is important to investigate the changes in the phenomenology of broken supersymmetry which results from the changes in the composition of neutralinos and charginos that may arise because of the changes in the pattern of soft gaugino masses at the grand unification scale [21]. The consequences of nonuniversal gaugino masses at the grand unified scale and the resulting change in boundary conditions has been considered in several papers. This includes the study of constraints arising from different experimental measurements [22–24], and in the study of supersymmetric dark matter candidates [25, 26].

One of the major goals of high energy colliders is to discover the supersymmetric partners of the Standard Model particles. In particular, a high energy e^+e^- linear collider with a center-of-mass energy of $\sqrt{s} = 500$ GeV in the first stage, and with a high luminosity $\mathcal{L} = 500 \text{ fb}^{-1}$, will be important in determining the parameters of the broken supersymmetric model with a high precision [27–31].

Recently in [17, 32] a detailed study of the radiative production of neutralinos in electron-positron collisions in low energy supersymmetric models with universal gaugino masses at the grand unified scale has been carried out. In this paper we shall carry out a study of the implications of the nonuniversal gaugino masses, as they arise in grand unified theories, for the production of lightest neutralinos in electron-positron collisions. Since in a large class of models of supersymmetry the lightest neutralino is expected to be the lightest supersymmetric particle, it is one of the first states to be produced at the colliders. At an electron-positron collider, such as the International Linear Collider (ILC), the lightest neutralino can be directly produced in pairs [5, 33]. In collider experiments it will escape detection such that the direct production of the lightest neutralino pair is invisible.

One must, therefore, look for the signature of neutralinos in electron-positron colliders in the radiative production process

$$e^+ + e^- \rightarrow \tilde{\chi}_1^0 + \tilde{\chi}_1^0 + \gamma. \quad (\text{I.1})$$

The signature of this process is a single high energy photon with missing energy carried away by the neutralinos. In this paper we carry out a detailed study of the process (I.1) in supersymmetric grand unified theories with nonuniversal boundary conditions at the grand unified scale. Note that this process is suppressed by the square of the electromagnetic coupling. However, it might be the first process where the lightest supersymmetric particles could be observed at e^+e^- colliders. The process (I.1) has been studied in detail in the minimal supersymmetric model [34–44], in various approximations. Calculations have also been carried out for MSSM using general neutralino mixing [42–44]. This process has also been studied in detail in the next-to-minimal supersymmetric model (NMSSM) [17, 32]. On the other hand different LEP collaborations [45–49] have studied the signature of radiative neutralino production in detail, but have found no deviations from the SM prediction. Thus, they have only been able to set bounds on the masses of supersymmetric particles [45–47, 49].

We recall that in the SM the radiative neutrino process

$$e^+e^- \rightarrow \nu + \bar{\nu} + \gamma, \quad (\text{I.2})$$

is the leading process with the same signature as (I.1). The cross section for the process (I.2) depends on the number N_ν of light neutrino species [50]. This process acts as a main background to the radiative neutralino production process (I.1). There is also a supersymmetric background to the process (I.1) coming from radiative sneutrino production

$$e^+e^- \rightarrow \tilde{\nu} + \tilde{\nu}^* + \gamma. \quad (\text{I.3})$$

We shall consider both these processes as well, since they form the main background to the radiative process (I.1).

The layout of the paper is as follows. In Sec. II, we review different patterns of gaugino masses that arise in grand unified theories. We will consider grand unified theories based on $SU(5)$ and $SO(10)$ gauge groups, and discuss the origin of nonuniversal gaugino masses in these models. Here we also calculate the elements of the mixing matrix which are relevant for obtaining the couplings of the lightest neutralino to the electron, selectron, and Z boson which control the radiative neutralino production process (I.1). Furthermore, we also describe in detail the typical set of input parameters that are used in our numerical evaluation of cross sections. The set of parameters that we use are obtained by imposing various experimental and theoretical constraints discussed in Appendix B on the parameter space of the minimal supersymmetric standard model with underlying grand unification. These constraints will also be used throughout to arrive at the allowed parameter space for different models in this paper.

Furthermore, we expect low energy observables from flavor physics and $g - 2$ to have some impact in constraining various models studied in this paper. The study of the impact of these observables on our analysis is, however, beyond the scope of present paper.

In Sec. III we summarize the phase space for the signal process, and also the cuts on the photon angle and energy that are used to regularise the infrared and collinear divergences in the tree level cross section. In Sec. IV we evaluate the cross section for the signal process (I.1) in different grand unified theories with nonuniversal gaugino masses, using the set of parameters obtained in Sec. II for different patterns of gaugino mass parameters at the grand unified scale. We have included higher order QED radiative corrections in our calculations. We also compare and contrast the results so obtained with the corresponding cross section in the MSSM with universal gaugino masses at the grand unified scale. The dependence of the cross section on the parameters of the neutralino sector, and on the selectron masses is also studied numerically.

In Sec. V we discuss the backgrounds to the radiative neutralino production process (I.1) from the SM and supersymmetric processes. An excess of photons from radiative neutralino production over the backgrounds measured through statistical significance is also discussed here and calculated for different grand unified models. Our results are summarized and the conclusions presented in Sec. VI.

II. GAUGINO MASS PATTERNS IN GRAND UNIFIED THEORIES

In this section we shall discuss soft supersymmetry breaking gaugino mass patterns that arise in $SU(5)$ and $SO(10)$ supersymmetric grand unified models, and the implications of these mass patterns for the neutralino masses and couplings. In Appendix A, we summarize our notations for the neutralino mass matrix and the couplings of the lightest neutralino that are relevant to our study[17, 51]. Furthermore, in Appendix B we summarize the current experimental constraints [52–55] on the parameters of the neutralino mass matrix that we use in our calculations.

A. Universal Gaugino Masses in Grand Unified Theories

In supersymmetric models, with gravity mediated supersymmetry breaking, usually denoted as mSUGRA, the soft supersymmetry breaking gaugino mass parameters M_1 , M_2 , and M_3 and the respective gauge couplings g_i satisfy the renormalization group equations (RGEs) ($|M_3| \equiv M_{\tilde{g}}$, the gluino mass)

$$16\pi^2 \frac{dM_i}{dt} = 2b_i M_i g_i^2, \quad b_i = \left(\frac{33}{5}, 1, -3 \right), \quad (\text{II.1})$$

$$16\pi^2 \frac{dg_i}{dt} = b_i g_i^3 \quad (\text{II.2})$$

at the one-loop order, where $i = 1, 2, 3$ refer to the $U(1)_Y$, $SU(2)_L$ and the $SU(3)$ gauge groups, respectively. Here, $g_1 = \frac{5}{3}g'$, $g_2 = g$, with g' and g as $U(1)_Y$ and $SU(2)_L$ gauge couplings, respectively, and g_3 is the $SU(3)_C$ gauge coupling. With the universal boundary conditions on the gaugino masses ($\alpha_i = g_i^2/4\pi$, $i = 1, 2, 3$), we have

$$M_1 = M_2 = M_3 = m_{1/2}, \quad (\text{II.3})$$

$$\alpha_1 = \alpha_2 = \alpha_3 = \alpha_G, \quad (\text{II.4})$$

at the GUT scale M_G . Then the RGEs (II.1) and (II.2) imply that the soft gaugino masses scale like gauge couplings:

$$\frac{M_1(M_Z)}{\alpha_1(M_Z)} = \frac{M_2(M_Z)}{\alpha_2(M_Z)} = \frac{M_3(M_Z)}{\alpha_3(M_Z)} = \frac{m_{1/2}}{\alpha_G}. \quad (\text{II.5})$$

The relation (II.5) implies that out of three gaugino mass parameters only one is independent, which we are free to choose as the gluino mass $M_{\tilde{g}}$. The remaining soft gaugino mass parameters can be determined through

$$M_1(M_Z) = \frac{5\alpha}{3\alpha_3 \cos^2 \theta_W} M_{\tilde{g}} \simeq 0.14 M_{\tilde{g}}, \quad (\text{II.6})$$

$$M_2(M_Z) = \frac{\alpha}{\alpha_3 \sin^2 \theta_W} M_{\tilde{g}} \simeq 0.28 M_{\tilde{g}}, \quad (\text{II.7})$$

where we have used the values of various couplings at the Z^0 to be

$$\alpha^{-1}(M_Z) = 127.9, \quad \sin^2 \theta_W = 0.23, \quad \alpha_3(M_Z) = 0.12. \quad (\text{II.8})$$

For the gaugino mass parameters this leads to the ratio

$$M_1 : M_2 : M_3 \simeq 1 : 2 : 7.1. \quad (\text{II.9})$$

The gaugino mass parameters described above are the running masses evaluated at the electroweak scale M_Z .

Using the ratio (II.9) and the constraint (B.3), we have the lower bound on the parameter M_1

$$M_1 \gtrsim 50 \text{ GeV}, \quad (\text{II.10})$$

in mSUGRA model. We shall implement this constraint on the parameter M_1 in our calculations.

For the case of universal gaugino masses at the grand unified scale, we shall use the set of parameters shown in Table I. We shall call this set of parameters the MSSM electroweak symmetry breaking scenario (EWSB) [56]. This scenario has the advantage that it allows us to study the dependence of the neutralino masses and the radiative neutralino production cross section on μ and M_2 , and on the selectron masses.

The values of different parameters in Table I have been arrived as follows. We first choose the smallest value of M_3 to be around 1400 GeV as dictated by the experimental constraints on the gluino mass. We then vary it from 1400 to 3000 GeV in steps of 100 GeV. For the smallest value of $M_3 = 1400$ GeV, we determine the values of soft gaugino mass parameters M_1 and M_2 . Increasing the value of M_3 in steps of 100 GeV, we obtain the corresponding values of M_1 and M_2 for different values of M_3 . This is shown in Fig. 1 as the curve labelled MSSM EWSB. Then we scan the values of the parameter M_2 , corresponding to different values of M_3 , with values of the parameter μ varying between 110 to 200 GeV such that the mass of the lightest neutralino lies between 100 to 200 GeV. This is shown as contour plot in Fig. 2. For Table I for the MSSM EWSB, we have chosen the values of M_2 and μ in Fig. 2 which correspond to the lightest neutralino mass of 108 GeV and chargino mass larger than 110 GeV. Other values can be obtained by choosing a higher mass for the lightest neutralino.

After selecting the values of the parameters for our analysis, we vary the value of $\tan \beta$ in the range so that the top and bottom quark Yukawa couplings remain perturbative upto the grand unified scale. For this variation in the value of $\tan \beta$, we find that the mass of the lightest neutralino varies by only $\pm (2 - 3)$ GeV compared to its value for $\tan \beta = 10$, with very little change in the cross section for the radiative neutralino production. Since our analysis is insensitive to the value of $\tan \beta$, we have chosen $\tan \beta = 10$ for definiteness.

We note from the Appendix A, the couplings of the lightest neutralino to electrons, selectrons, and Z bosons, which are used for the calculation of the radiative neutralino production cross section, are determined by the corresponding elements of the neutralino mixing matrix N_{ij} . For the MSSM EWSB scenario of Table I the composition of the lightest neutralino is given by

$$N_{1j} = (0.345, -0.175, 0.703, -0.596). \quad (\text{II.11})$$

$f_{ab}(\Phi)$ can be written as

$$f_{ab}(\Phi) = f_0(\Phi^s)\delta_{ab} + \sum_n f_n(\Phi^s)\frac{\Phi_{ab}^n}{M_P} + \dots \quad (\text{II.13})$$

Here Φ^s and the Φ^n denote the singlet and the non-singlet chiral superfields, respectively. Also, $f_0(\Phi^s)$ and $f_n(\Phi^s)$ are functions of gauge singlet superfields Φ^s , and M_P denotes some large scale, e.g. the Planck scale. When the auxiliary part F_Φ of a chiral superfield Φ in $f(\Phi)$ gets a VEV $\langle F_\Phi \rangle$, the interaction (II.12) gives rise to soft gaugino masses:

$$\mathcal{L}_{g.k.} \supset \frac{\langle F_\Phi \rangle_{ab}}{M_P} \lambda^a \lambda^b + h.c., \quad (\text{II.14})$$

where $\lambda^{a,b}$ are gaugino fields. Here, we have denoted by λ^1 , λ^2 and λ^3 as the $U(1)$, $SU(2)$ and $SU(3)$ gaugino fields, respectively. Since the gauginos belong to the adjoint representation of the gauge group, Φ and F_Φ can belong to any of the representations appearing in the symmetric product of the two adjoint representations of corresponding gauge group.

Since the SM can be embedded into a larger gauge group the question of unified gauge group needs to be discussed in order to study the implications for nonuniversal soft gaugino masses in grand unified theories. We recall that there is chain of group embeddings of the SM gauge group into a larger group [57]

$$SU(3)_C \times SU(2)_L \times U(1)_Y \subset SU(5) \subset SO(10) \subset E_6 \subset E_7 \subset E_8. \quad (\text{II.15})$$

However, we note that in four-dimensional grand unified theories the gauge groups E_7 and E_8 do not lead to a chiral structure of the weak interactions, and hence are ruled out as grand unified gauge groups on phenomenological grounds. This leaves out only the three groups, $SU(5)$, $SO(10)$, and E_6 as possible grand unified gauge groups in four dimensions. Here we shall study the implications of nonuniversal gaugino masses in the case of $SU(5)$ and $SO(10)$ grand unified gauge groups.

1. $SU(5)$

In this Section we shall consider the case of embedding of the SM gauge group into the grand unified gauge group $SU(5)$. In the symmetric product of the two adjoint (**24** dimensional) representations of $SU(5)$, we have

$$(\mathbf{24} \otimes \mathbf{24})_{\text{Symm}} = \mathbf{1} \oplus \mathbf{24} \oplus \mathbf{75} \oplus \mathbf{200}. \quad (\text{II.16})$$

In the simplest case where Φ and F_Φ are assumed to be in the singlet representation of $SU(5)$, we have equal gaugino masses at the GUT scale. But, as we can see from (II.16), Φ and F_Φ can belong to any of the non-singlet representations **24**, **75**, and **200** of $SU(5)$. In such cases the soft gaugino masses are unequal but related to one another via the representation invariants of the gauge group [21]. In Table II we show the ratios of gaugino masses which result when F_Φ belongs to different representations of $SU(5)$ in the decomposition (II.16). In this paper, for definiteness, we shall study the case of each representation independently, although an arbitrary combination of these is also allowed.

In the one-loop approximation, the solution of renormalization group (RG) equations for the soft supersymmetry breaking gaugino masses M_1 , M_2 , and M_3 can be written as [58]

$$\frac{M_i(t)}{\alpha_i(t)} = \frac{M_i(\text{GUT})}{\alpha_i(\text{GUT})}, \quad i = 1, 2, 3. \quad (\text{II.17})$$

Then at any arbitrary scale we have :

$$M_1 = \frac{5}{3} \frac{\alpha}{\cos^2 \theta_W} \left(\frac{M_1(\text{GUT})}{\alpha_1(\text{GUT})} \right), \quad M_2 = \frac{\alpha}{\sin^2 \theta_W} \left(\frac{M_2(\text{GUT})}{\alpha_2(\text{GUT})} \right), \quad M_3 = \alpha_3 \left(\frac{M_3(\text{GUT})}{\alpha_3(\text{GUT})} \right). \quad (\text{II.18})$$

With these results, we can write the gaugino masses for the **24** dimensional representation of $SU(5)$ as

$$\frac{M_1}{M_3} = -\frac{1}{2} \left(\frac{5}{3} \frac{\alpha}{\cos^2 \theta_W} \right) \left(\frac{1}{\alpha_3} \right), \quad \frac{M_2}{M_3} = -\frac{3}{2} \left(\frac{\alpha}{\sin^2 \theta_W} \right) \left(\frac{1}{\alpha_3} \right). \quad (\text{II.19})$$

$SU(5)$	M_1^G	M_2^G	M_3^G	M_1^{EW}	M_2^{EW}	M_3^{EW}
1	1	1	1	1	2	7.1
24	1	3	-2	1	6	-14.3
75	1	$-\frac{3}{5}$	$-\frac{1}{5}$	1	-1.18	-1.41
200	1	$\frac{1}{5}$	$\frac{1}{10}$	1	0.4	0.71

TABLE II: Ratios of the gaugino masses at the GUT scale in the normalization $M_1(GUT) = 1$, and at the electroweak scale in the normalization $M_1(EW) = 1$ for F -terms in different representations of $SU(5)$. These results are obtained by using 1-loop renormalization group equations.

Similarly, for the **75** dimensional representation of $SU(5)$, we have the result

$$\frac{M_1}{M_3} = -5 \left(\frac{5}{3} \frac{\alpha}{\cos^2 \theta_W} \right) \left(\frac{1}{\alpha_3} \right), \quad \frac{M_2}{M_3} = 3 \left(\frac{\alpha}{\sin^2 \theta_W} \right) \left(\frac{1}{\alpha_3} \right), \quad (\text{II.20})$$

and finally for the **200** dimensional representation of $SU(5)$ we have

$$\frac{M_1}{M_3} = 10 \left(\frac{5}{3} \frac{\alpha}{\cos^2 \theta_W} \right) \left(\frac{1}{\alpha_3} \right), \quad \frac{M_2}{M_3} = 2 \left(\frac{\alpha}{\sin^2 \theta_W} \right) \left(\frac{1}{\alpha_3} \right). \quad (\text{II.21})$$

To compute the ratios of the gaugino masses at the electroweak (EW) scale M_Z for different representations of $SU(5)$ in the product (II.16), we use the relevant renormalization group equations for the soft gaugino masses. In Table II we show the approximate results for these masses at the electroweak scale $M_i(EW)$. These are calculated using one loop renormalization group equations for the gaugino masses and the gauge couplings. The effect of two-loop calculations is to increase the ratio M_1/M_2 by an amount which is not significant. It is important to note that these results are consistent with the unification of gauge couplings

$$\alpha_3^G = \alpha_2^G = \alpha_1^G = \alpha^G (\approx 1/25), \quad (\text{II.22})$$

at the GUT scale, where we have neglected the contribution of non universality in gaugino masses to the gauge couplings, which is not significant.

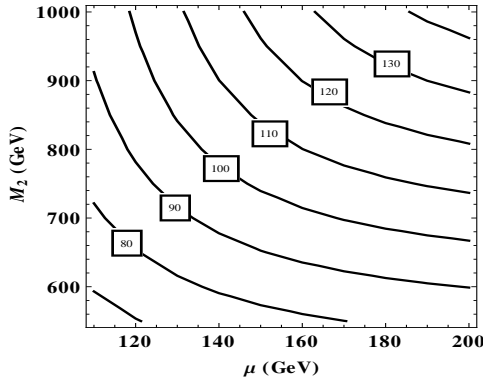


FIG. 3: The lightest neutralino mass in $\mu - M_2$ plane for $SU(5)$ with Φ and F_Φ in the **24** dimensional representation. The value of μ giving $m_{\tilde{\chi}_1^0} \approx 108$ GeV, for the smallest value of M_2 satisfying the gluino mass constraint, is chosen for our analyses.

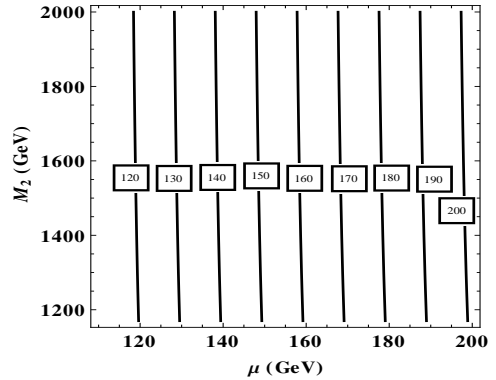


FIG. 4: The lightest neutralino mass in $\mu - M_2$ plane for $SU(5)$ with Φ and F_Φ in the **75** dimensional representation. The value of μ giving $m_{\tilde{\chi}_1^0} \approx 108$ GeV, for the smallest value of M_2 satisfying the gluino mass constraint, is chosen for our analyses.

The input parameters for **24**, **75** and **200** dimensional representations of $SU(5)$ in Table II are chosen in a manner similar to the one we used for the parameter space of MSSM EWSB. The lowest values of M_1 and M_2

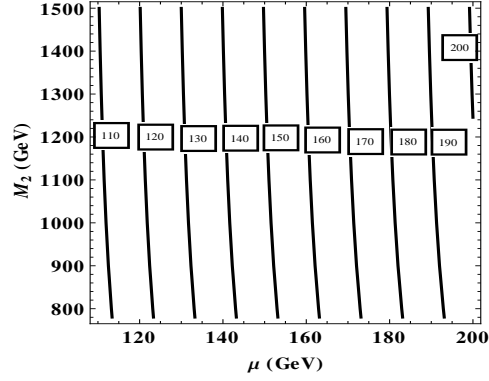


FIG. 5: The lightest neutralino mass in $\mu - M_2$ plane for $SU(5)$ with Φ and F_Φ in the **200** dimensional representation. The value of μ giving $m_{\chi_1^0} \approx 108$ GeV, for the smallest value of M_2 satisfying the gluino mass constraint, is chosen for our analyses.

$\tan \beta = 10$	$\mu = 138$ GeV	$M_1 = 149$ GeV	$M_2 = 890$ GeV
$M_3 = -2121$ GeV	$A_t = -1000$ GeV	$A_b = -2050$ GeV	$A_\tau = -2050$ GeV
$m_{\chi_1^0} = 108$ GeV	$m_{\chi_1^\pm} = 138.5$ GeV	$m_{\tilde{e}_R} = 156$ GeV	$m_{\tilde{\nu}_e} = 136$ GeV
$m_{\chi_2^0} = 146$ GeV	$m_{\chi_2^\pm} = 903$ GeV	$m_{\tilde{e}_L} = 157$ GeV	$m_h = 123.5$ GeV

TABLE III: Input parameters and resulting masses for various states in $SU(5)$ supersymmetric grand unified theory with Φ and F_Φ in the **24** dimensional representation.

We shall refer to this model as $[SU(5)]_{24}$ in the text.

satisfying the gluino mass constraint are chosen from Fig. 1 corresponding to various $SU(5)$ representations shown there. We then plot the values of M_2 versus μ for various representations in contour plots shown in Figs. 3, 4 and 5. The values of M_2 and μ are then selected which result in the lightest neutralino mass of 108 GeV and chargino mass larger than 110 GeV. For $SU(5)_{75}$ and $SU(5)_{200}$ the bino and wino mass parameters $M_1, M_2 \gg \mu$, therefore the LSP mass in these cases is almost equal to μ . This is seen from Figs. 4 and 5, where the contours in the $M_2 - \mu$ plane are independent of M_2 .

The input parameters and the resulting masses for the **24**, **75**, and **200** dimensional representations of $SU(5)$ which result in nonuniversal gaugino masses at the grand unified scale obtained in a manner described above are shown in Tables III, IV and V, respectively. In arriving at the parameter values in these Tables, we have taken into account various theoretical and phenomenological constraints, including the electroweak symmetry breaking at the correct scale, as described in the Appendix B. Other values can be obtained by choosing larger values of the parameter M_3 .

The composition of the lightest neutralino for the different representations of $SU(5)$ in Table II is obtained from the mixing matrix for the choices of parameters given in Tables III, IV and V. This composition is calculated to be:

1. $SU(5)$ with Φ and F_Φ in the **24** dimensional representation (labelled as model $[SU(5)]_{24}$):

$$N_{1j} = (0.638, -0.054, 0.598, -0.482); \quad (\text{II.23})$$

$\tan \beta = 10$	$\mu = 108$ GeV	$M_1 = 993$ GeV	$M_2 = -1172$ GeV
$M_3 = -1400$ GeV	$A_t = 1000$ GeV	$A_b = 2300$ GeV	$A_\tau = 2300$ GeV
$m_{\chi_1^0} = 108$ GeV	$m_{\chi_1^\pm} = 109$ GeV	$m_{\tilde{e}_R} = 156$ GeV	$m_{\tilde{\nu}_e} = 136$ GeV
$m_{\chi_2^0} = 110$ GeV	$m_{\chi_2^\pm} = 1916$ GeV	$m_{\tilde{e}_L} = 157$ GeV	$m_h = 123.5$ GeV

TABLE IV: Input parameters and resulting masses for various states in $SU(5)$ supersymmetric grand unified theory with Φ and F_Φ in the **75** dimensional representation.

We shall refer to this model as $[SU(5)]_{75}$ in the text.

$\tan \beta = 10$	$\mu = 111 \text{ GeV}$	$M_1 = 1970 \text{ GeV}$	$M_2 = 788 \text{ GeV}$
$M_3 = 1399 \text{ GeV}$	$A_t = 1000 \text{ GeV}$	$A_b = 2300 \text{ GeV}$	$A_\tau = 2300 \text{ GeV}$
$m_{\chi_1^0} = 107.7 \text{ GeV}$	$m_{\chi_1^\pm} = 111 \text{ GeV}$	$m_{\tilde{e}_R} = 166 \text{ GeV}$	$m_{\tilde{\nu}_e} = 136 \text{ GeV}$
$m_{\chi_2^0} = 117 \text{ GeV}$	$m_{\chi_2^\pm} = 807 \text{ GeV}$	$m_{\tilde{e}_L} = 157 \text{ GeV}$	$m_h = 123.7 \text{ GeV}$

TABLE V: Input parameters and resulting masses for various states in $SU(5)$ supersymmetric grand unified theory with Φ and F_Φ in the **200** dimensional representation.

We shall refer to this model as $[SU(5)]_{200}$ in the text.

2. $SU(5)$ with Φ and F_Φ in the **75** dimensional representation (labelled as model $[SU(5)]_{75}$):

$$N_{1j} = (0.031, 0.056, -0.710, -0.700); \quad (\text{II.24})$$

3. $SU(5)$ with Φ and F_Φ in the **200** dimensional representation (labelled as model $[SU(5)]_{200}$):

$$N_{1j} = (0.018, -0.085, 0.719, -0.689). \quad (\text{II.25})$$

We note from (II.23), (II.24), and (II.25) that for the **24** dimensional representation of $SU(5)$, the dominant component of the neutralino is the bino, whereas for the other representations of $SU(5)$, there is a higgsino like lightest neutralino. Thus, for **75** and **200** dimensional representations the neutralino being higgsino like couples weakly to the selectron, with the dominant contribution to the cross section coming from the neutralino- Z^0 coupling.

2. $SO(10)$

We now consider the embedding of the SM gauge group in a $SO(10)$ supersymmetric grand unified theory. Since the adjoint representation of $SO(10)$ is **45** dimensional, Φ and F_Φ can belong to any of the following representations appearing [59] in the symmetric product of two **45** dimensional representations of $SO(10)$:

$$(\mathbf{45} \times \mathbf{45})_{\text{Symm}} = \mathbf{1} \oplus \mathbf{54} \oplus \mathbf{210} \oplus \mathbf{770}. \quad (\text{II.26})$$

There are three maximal proper subgroups of $SO(10)$ which are consistent with the fermion content of the Standard Model. These are (i) $SU(5) \subset SO(10)$ with the normal (nonflipped) embedding; (ii) $SU(5)' \times U(1) \subset SO(10)$ with the flipped embedding; and (iii) $SU(4) \times SU(2)_L \times SU(2)_R \subset SO(10)$ embedding. Using relations (II.17) and (II.18), we obtain the gaugino mass parameters at the GUT scale for different representations that arise in the symmetric product of two adjoint representations of $SO(10)$ with the relevant embedding of the SM gauge group in $SO(10)$. These are shown in Tables VI, VII, and VIII. The ratio of the gaugino masses at the GUT scale for the different cases for $SO(10)$ shown in these Tables can be scaled down to the electroweak scale, as described above. The results for the gaugino masses at the electroweak scale for these cases are also shown in Tables VI, VII, and VIII.

We note from Table VI that the ratios of gaugino masses for the different representations of $SO(10)$ in the symmetric product (II.26) with the unflipped embedding $SU(5) \subset SO(10)$ are identical to the corresponding gaugino mass ratios in Table II for the embedding of SM in $SU(5)$. Therefore, the input parameters and the resulting masses for the gaugino mass ratios in Table VI for $SO(10)$ are identical to the corresponding Tables III, IV, and V for $SU(5)$.

On the other hand, for the flipped embedding $SU(5)' \times U(1) \subset SO(10)$, Table VII, the gaugino mass ratios for the **210** and **770** dimensional representations of the grand unified gauge group can be different from the corresponding ratios for $SU(5)$.

In the case of $SO(10)$ we choose the parameter values in a manner similar to the case of MSSM EWSB and the $SU(5)$ grand unified theory. The result of such a procedure is shown in Fig. 1, and in Figs.6, 7 and 8. The resulting values of parameters are shown in Tables IX, X and XI.

We note that the ratio of the gaugino masses for the **(24, 0)**, **(75, 0)** of the **210** dimensional representation of $SO(10)$, and **(75, 0)**, **(200, 0)** of the **770** representation of $SO(10)$ follow the same pattern as the **(24, 0)** of the **54** dimensional representation of $SO(10)$. The behaviour of the cross section for the radiative neutralino cross section will be similar in these cases due to the fact that the dominant component of the lightest neutralino in this case is a bino. Similarly, the **(24, 0)** of the **770** dimensional representation of $SO(10)$ has the same pattern as **200** dimensional representation of $SU(5)$. Here also the behavior will be same. Because of this we shall

$SO(10)$	$SU(5)$	M_1^G	M_2^G	M_3^G	M_1^{EW}	M_2^{EW}	M_3^{EW}
1	1	1	1	1	1	2	7.1
54	24	1	3	-2	1	6	-14.3
210	1	1	1	1	1	2	7.1
	24	1	3	-2	1	6	-14.3
	75	1	$-\frac{3}{5}$	$-\frac{1}{5}$	1	-1.18	-1.41
	1	1	1	1	1	2	7.1
	24	1	3	-2	1	6	-14.3
770	75	1	$-\frac{3}{5}$	$-\frac{1}{5}$	1	-1.18	-1.14
	200	1	$\frac{1}{5}$	$\frac{1}{10}$	1	0.4	0.71

TABLE VI: Ratios of the gaugino masses at the GUT scale in the normalization $M_1(GUT) = 1$, and at the electroweak scale in the normalization $M_1(EW) = 1$ for F -terms in representations of $SU(5) \subset SO(10)$ with the normal (nonflipped) embedding. These results have been obtained at the 1-loop level.

$SO(10)$	$[SU(5)' \times U(1)]_{flipped}$	M_1^G	M_2^G	M_3^G	M_1^{EW}	M_2^{EW}	M_3^{EW}
1	(1,0)	1	1	1	1	2	7.1
54	(24,0)	1	3	-2	1	6	-14.3
210	(1,0)	1	$-\frac{5}{19}$	$-\frac{5}{19}$	1	-0.52	-1.85
	(24,0)	1	$-\frac{15}{7}$	$\frac{10}{7}$	1	-4.2	10
	(75,0)	1	-15	-5	1	-28	-33.33
	(1,0)	1	$\frac{5}{77}$	$\frac{5}{77}$	1	0.13	0.46
	(24,0)	1	$\frac{15}{101}$	$-\frac{10}{101}$	1	0.3	-0.70
770	(75,0)	1	-15	-5	1	-28	-33.3
	(200,0)	1	5	$\frac{5}{2}$	1	9.33	16.67

TABLE VII: Ratios of the gaugino masses at the GUT scale in the normalization $M_1(GUT) = 1$, and at the electroweak scale in the normalization $M_1(EW) = 1$ at the 1-loop level for F -terms in representations of flipped $SU(5)' \times U(1) \subset SO(10)$.

$SO(10)$	$SU(4) \times SU(2)_R$	M_1^G	M_2^G	M_3^G	M_1^{EW}	M_2^{EW}	M_3^{EW}
1	(1,1)	1	1	1	1	2	7.1
54	(1,1)	1	3	2	1	6	-14.3
210	(1,1)	1	$-\frac{5}{3}$	0	1	-3.35	0
	(15,1)	1	0	$-\frac{5}{4}$	1	0	-9.09
	(15,3)	1	0	0	1	0	0
	(1,1)	1	$\frac{25}{19}$	$\frac{10}{19}$	1	2.6	3.7
	(1,5)	1	0	0	1	0	0
770	(15,3)	1	0	0	1	0	0
	(84,1)	1	0	$\frac{5}{32}$	1	0	1.11

TABLE VIII: Ratios of the gaugino masses at the GUT scale in the normalization $M_1(GUT) = 1$, and at the electroweak scale in the normalization $M_1(EW) = 1$ at the 1-loop level for F -terms in representations of $SU(4) \times SU(2)_L \times SU(2)_R \subset SO(10)$.

$\tan \beta = 10$	$\mu = 116 \text{ GeV}$	$M_1 = 760 \text{ GeV}$	$M_2 = -395 \text{ GeV}$
$M_3 = -1405 \text{ GeV}$	$A_t = 1000 \text{ GeV}$	$A_b = 2300 \text{ GeV}$	$A_\tau = 2300 \text{ GeV}$
$m_{\chi_1^0} = 108 \text{ GeV}$	$m_{\chi_1^\pm} = 111 \text{ GeV}$	$m_{\tilde{e}_R} = 156 \text{ GeV}$	$m_{\tilde{\nu}_e} = 136 \text{ GeV}$
$m_{\chi_2^0} = 122 \text{ GeV}$	$m_{\chi_2^\pm} = 422 \text{ GeV}$	$m_{\tilde{e}_L} = 158 \text{ GeV}$	$m_h = 124.2 \text{ GeV}$

TABLE IX: Input parameters and resulting masses for various states in $SU(5)' \times U(1) \subset SO(10)$ supersymmetric grand unified theory with Φ and F_Φ in the **210** dimensional representation with $SU(5)' \times U(1)$ in (1,0) dimensional representation.

We shall refer to this model as $[SO(10)]_{210}$ in the text.

focus on the (1,0) option for the **210** and **770** dimensional representations in Table VII. Similarly, because of phenomenological reasons, we focus on the (1,1) of $SU(4) \times SU(2)_R$ of the **770** representation only.

For the parameters of Tables IX, X and XI the composition of the lightest neutralino is given by the following.

1. $SO(10)$ where $SU(5)' \times U(1) \subset SO(10)$ with Φ and F_Φ in the **210** dimensional representation with $SU(5)' \times U(1)$ in (1,0) dimensional representation (labelled as model $[SO(10)]_{210}$):

$$N_{1j} = (0.038, 0.194, -0.719, -0.666); \quad (\text{II.27})$$

2. $SO(10)$ where $SU(5)' \times U(1) \subset SO(10)$ with Φ and F_Φ in the **770** dimensional representation with

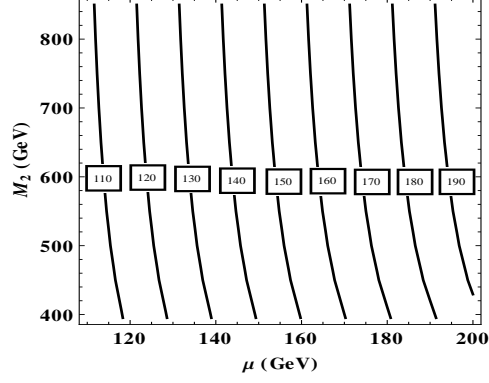


FIG. 6: The lightest neutralino mass in $\mu - M_2$ plane for $SO(10)$ where $SU(5)' \times U(1) \subset SO(10)$ with Φ and F_Φ in the **210** (II.27). The value of μ giving $m_{\tilde{\chi}_1^0} \approx 108$ GeV, for the selected value of M_2 is considered for our analyses.

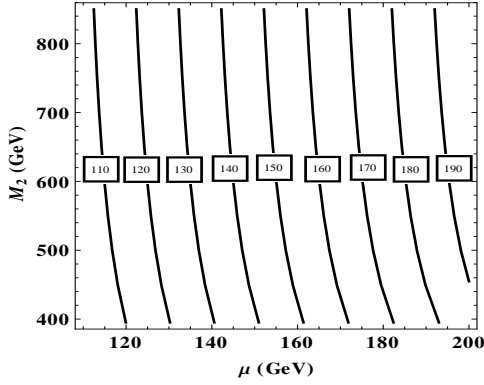


FIG. 7: The lightest neutralino mass in $\mu - M_2$ plane for $SO(10)_{770}$ scenario. The value of μ giving $m_{\tilde{\chi}_1^0} \approx 108$ GeV, for the smallest value of M_2 satisfying the gluino mass constraint, is chosen for our analyses.

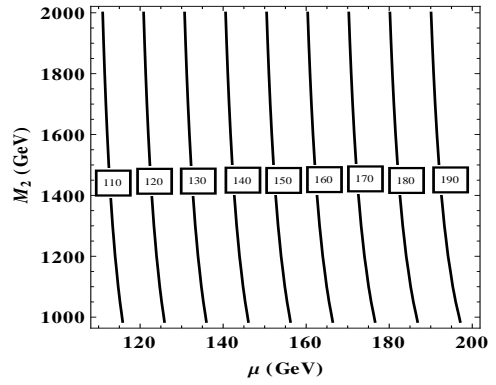


FIG. 8: The lightest neutralino mass in $\mu - M_2$ plane for $SO(10)_{770'}$ scenario. The value of μ giving $m_{\tilde{\chi}_1^0} \approx 108$ GeV, for the smallest value of M_2 satisfying the gluino mass constraint, is chosen for our analyses.

$SU(5)' \times U(1)$ in $(\mathbf{1}, \mathbf{0})$ dimensional representation (labelled as model $[SO(10)]_{770}$):

$$N_{1j} = (0.011, -0.193, 0.724, -0.663); \quad (\text{II.28})$$

3. $SO(10)$ where $SU(4) \times SU(2)_R \times SU(2)_L \subset SO(10)$ with Φ and F_Φ in the **770** dimensional representation with $SU(4) \times SU(2)_R$ in $(\mathbf{1}, \mathbf{1})$ dimensional representation (labelled as model $[SO(10)]_{770'}$):

$$N_{1j} = (0.125, -0.660, 0.721, -0.678), \quad (\text{II.29})$$

$\tan \beta = 10$	$\mu = 118$ GeV	$M_1 = 3038$ GeV	$M_2 = 395$ GeV
$M_3 = 1398$ GeV	$A_t = 1000$ GeV	$A_b = 2300$ GeV	$A_\tau = 2300$ GeV
$m_{\tilde{\chi}_1^0} = 108$ GeV	$m_{\tilde{\chi}_1^\pm} = 113$ GeV	$m_{\tilde{e}_R} = 156$ GeV	$m_{\tilde{\nu}_e} = 136$ GeV
$m_{\tilde{\chi}_2^0} = 125$ GeV	$m_{\tilde{\chi}_2^\pm} = 422$ GeV	$m_{\tilde{e}_L} = 157$ GeV	$m_h = 124$ GeV

TABLE X: Input parameters and resulting masses for various states in $SU(5)' \times U(1) \subset SO(10)$ supersymmetric grand unified theory with Φ and F_Φ in the **770** dimensional representation with $SU(5)' \times U(1)$ in $(\mathbf{1}, \mathbf{0})$ dimensional representation.

We shall refer to this model as $[SO(10)]_{770}$ in the text.

$\tan \beta = 10$	$\mu = 113 \text{ GeV}$	$M_1 = 378 \text{ GeV}$	$M_2 = 985 \text{ GeV}$
$M_3 = 1402 \text{ GeV}$	$A_t = 1000 \text{ GeV}$	$A_b = 2300 \text{ GeV}$	$A_\tau = 2300 \text{ GeV}$
$m_{\chi_1^0} = 107.4 \text{ GeV}$	$m_{\chi_1^\pm} = 114 \text{ GeV}$	$m_{\tilde{e}_R} = 156 \text{ GeV}$	$m_{\tilde{\nu}_e} = 136 \text{ GeV}$
$m_{\chi_2^0} = 120 \text{ GeV}$	$m_{\chi_2^\pm} = 1000 \text{ GeV}$	$m_{\tilde{e}_L} = 157 \text{ GeV}$	$m_h = 123.5 \text{ GeV}$

TABLE XI: Input parameters and resulting masses for various states in $SU(4) \times SU(2)_R \times SU(2)_L \subset SO(10)$ supersymmetric grand unified theory with Φ and F_Φ in the **770** dimensional representation with $SU(4) \times SU(2)_R$ in **(1,1)** dimensional representation. We shall refer to this model as $[SO(10)]_{770'}$ in the text.

implying thereby that higgsino is the dominant component for the **210** and **770** dimensional representations with the embedding $SU(5)' \times U(1) \subset SO(10)$ and for the **770** dimensional representation with the embedding $SU(4) \times SU(2)_R \times SU(2)_L \subset SO(10)$. From the Figs.6, 7 and 8 we see that, because the lightest neutralino is dominantly a higgsino, the contours are almost independent of M_2 .

Thus, in these cases the dominant contribution to the radiative neutralino production cross section will come from the neutralino- Z^0 coupling. Since the LSP for most of the scenarios considered here has a dominant higgsino component, the Z^0 width imposes a strict constraint, as the Z^0 decay rate involves coupling to the higgsino component of the neutralino. We have imposed the LEP constraint on the anomalous Z^0 decay width in our calculations :

$$\Gamma(Z \rightarrow \tilde{\chi}_1^0 \tilde{\chi}_1^0) < 3\text{MeV}. \quad (\text{II.30})$$

III. RADIATIVE NEUTRALINO PRODUCTION IN GRAND UNIFIED THEORIES

In this Section We shall calculate the cross section for the radiative neutralino production process

$$e^-(p_1) + e^+(p_2) \rightarrow \tilde{\chi}_1^0(k_1) + \tilde{\chi}_1^0(k_2) + \gamma(q), \quad (\text{III.1})$$

in $SU(5)$ and $SO(10)$ grand unified theories with nonuniversal gaugino masses at the grand unified scale. The symbols in the brackets denote the four momenta of the corresponding particles. At the tree level, the Feynman diagrams contributing to the radiative neutralino production process are shown in Fig. 9. In order to calculate the cross section for the radiative process (III.1), we require the couplings of the neutralinos to electrons, the selectrons, and to the Z^0 bosons. These couplings are obtained from the neutralino mixing matrix (A.2) as in the Appendix A, with the values of the soft SUSY breaking gaugino mass parameters M_1 and M_2 for the respective grand unified theory, as calculated in Section II.

The elements of the neutralino mixing matrix N_{1j} for the case of $SU(5)$ and $SO(10)$, which are relevant for our calculations, were calculated in the previous section. As indicated earlier, as a benchmark, we shall calculate the radiative neutralino cross section for the MSSM with universal boundary condition (II.3) for the gaugino mass parameters at the GUT scale, for which we will work with the parameters in the MSSM electroweak symmetry breaking scenario (EWSB) [56]. This set of parameters is summarized in Table I. The relevant elements of the neutralino mixing matrix N_{1j} are summarized in (II.11).

A. Cross Section for the Signal Process

From Fig. 9, we see that the t - and u -channel exchange of right and left selectrons $\tilde{e}_{R,L}$, and via Z boson exchange in the s channel contribute to the process (III.1). The differential cross section for the process (III.1) can be written as [36, 60]

$$d\sigma = \frac{1}{2} \frac{(2\pi)^4}{2s} \prod_f \frac{d^3 \mathbf{p}_f}{(2\pi)^3 2E_f} \delta^{(4)}(p_1 + p_2 - k_1 - k_2 - q) |\mathcal{M}|^2, \quad (\text{III.2})$$

where \mathbf{p}_f and E_f are the final three-momenta \mathbf{k}_1 , \mathbf{k}_2 , \mathbf{q} and the final energies $E_{\chi_1^0}$, $E_{\chi_2^0}$, and E_γ of the neutralinos and the photon, respectively. Using the standard technique, we average over initial spins and sum over the spins of the outgoing neutralinos. We also sum over the polarizations of the outgoing photon. Putting all this into effect, the squared matrix element $|\mathcal{M}|^2$ in (III.2) can be written as [36]

$$|\mathcal{M}|^2 = \sum_{i \leq j} T_{ij}, \quad (\text{III.3})$$

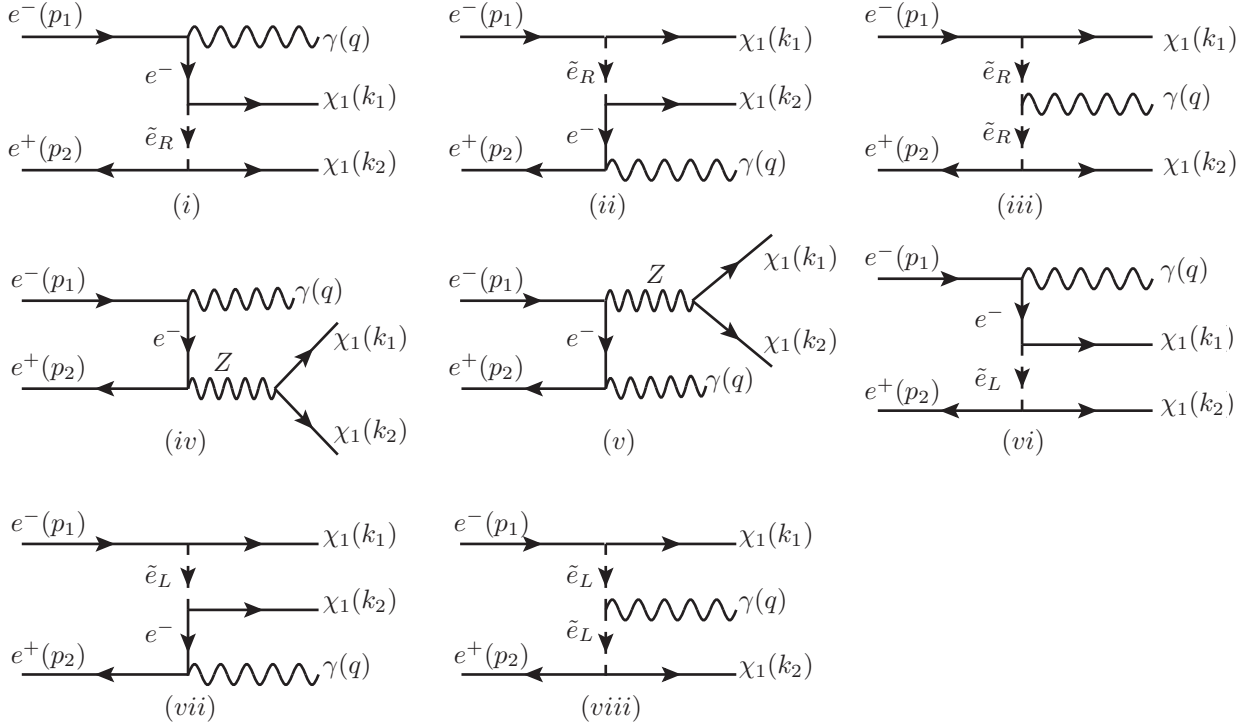


FIG. 9: Feynman diagrams contributing to the radiative neutralino production $e^+e^- \rightarrow \tilde{\chi}_1^0 \tilde{\chi}_1^0 \gamma$. There are six other diagrams which are exchange diagrams corresponding to (i, ii, iii, vi, vii, viii), with u -channel exchange of selectrons, wherein the neutralinos are crossed in the final state.

where T_{ij} are squared amplitudes corresponding to the Feynman diagrams in Fig. 9. The phase space for the radiative neutralino production process in (III.2) is described in detail in [36].

B. Radiative Corrections

The next generation linear colliders are designed to have a high luminosity, which in turn will require beams with bunches of high densities. Due to the above requirement of high number density in the bunch, there arise problems with the generation of strong electromagnetic fields in and around the bunches. This in turn generates initial state radiation (ISR) and beamstrahlung effects. These effects have been studied extensively in the past [61–64] in the context of the future linear colliders. Therefore ISR and beamstrahlung effects have to be considered in any realistic calculation of the cross sections at a future linear collider since they result in the loss of beam energy along with the disturbance of the initial beam calibration.

The majority of the emitted photons are soft and are lost down the beam pipe. Only the hard photons can be tagged. The radiated hard photon usually carries from the radiating particle a certain amount of energy, resulting in the energy distribution of the initial beams. So a precise knowledge of ISR along with distribution of the photon spectrum resulting from beamstrahlung and the behaviour of the electrons, positrons after the emission is required. We have calculated the radiative effects for our process and the background processes using CalcHEP [56], with parameters given in Table XII [65]. The resulting spectrum of electrons has been calculated using the structure function of the initial leptons valid upto all orders in perturbation theory. We note that the radiative effects are included in all our calculations of the signal and background processes.

IV. NUMERICAL RESULTS

The tree-level cross section for radiative neutralino production (III.1), and the standard model background from radiative neutrino and sneutrino production, (I.2) and (I.3), have been calculated using the program CalcHEP [56]. As noted above we have included the effects of radiative corrections to the signal as well as the

Collider Parameters	ILC
σ_x (nm)	640
σ_y (nm)	5.7
σ_z (μm)	300
N (10^{10})	2

TABLE XII: Beam parameters for the ILC, where N is the number of particles in the bunch and σ_x , σ_y are the transverse bunch sizes at the interaction point, with σ_z as the bunch length.

\sqrt{s}	σ_{EWSB}	$\sigma_{EWSB} + R.E.$	σ_{SM}	$\sigma_{SM} + R.E.$
GeV	(fb) $\times 10^{-1}$	(fb) $\times 10^{-1}$	(fb) $\times 10^3$	(fb) $\times 10^3$
300	0.9072	0.7586	2.1899	2.4187
400	1.4035	1.2821	2.3691	2.4373
500	1.3963	1.3377	2.4191	2.4321
600	1.2540	1.2383	2.4329	2.4518
700	1.0922	1.1030	2.4226	2.4359
800	0.9443	0.9721	2.3980	2.3648
900	0.8179	0.8568	2.3687	2.3318
1000	0.7124	0.7576	2.3341	2.2934

TABLE XIII: Cross section of the signal process in MSSM EWSB scenario, along with the the SM irreducible background with and without the inclusion of the radiative effects (R.E.) due to ISR and beamstrahlung.

background processes. We recall that the tree level cross sections have infrared and collinear divergences, which must be regularized by imposing cuts on the fraction of beam energy carried by the photon and the scattering angle of the photon [36]. To implement this regularization, we define the fraction of the beam energy carried by the photon as $x = E_\gamma/E_{\text{beam}}$, where $\sqrt{s} = 2E_{\text{beam}}$ is the center of mass energy, and E_γ is the energy carried away by the photon. We then impose the following cuts on x , and on the scattering angle θ_γ of the photon [66]:

$$0.02 \leq x \leq 1 - \frac{m_{\chi_1^0}^2}{E_{\text{beam}}^2}, \quad (\text{IV.1})$$

$$-0.95 \leq \cos \theta_\gamma \leq 0.95. \quad (\text{IV.2})$$

Note that the lower cut on x in (IV.1) corresponds to photon energy $E_\gamma = 5$ GeV for $\sqrt{s} = 500$ GeV. The upper bound of $(1 - m_{\chi_1^0}^2/E_{\text{beam}}^2)$ on x corresponds to the kinematical limit of radiative neutralino production process. The detector acceptance cut on the photon is applied so as to enhance the signal over the main irreducible background coming from the radiative neutrino production. We did not find any other cuts which would significantly reduce the background.

The mass of the lightest neutralino for MSSM, with universal boundary conditions on the gaugino mass parameters at the GUT scale is taken to be $m_{\chi_1^0} = 108$ GeV from the EWSB scenario, to implement the cuts on the photon energy in the calculation of the cross sections. Using Eq. (IV.1) we get a fixed upper limit $E_\gamma^{\text{max}} \simeq 203.3$ GeV for MSSM at $\sqrt{s} = 500$ GeV for the photon energy. We have used these cuts for both signal and background processes for all the scenarios that we have considered in this paper.

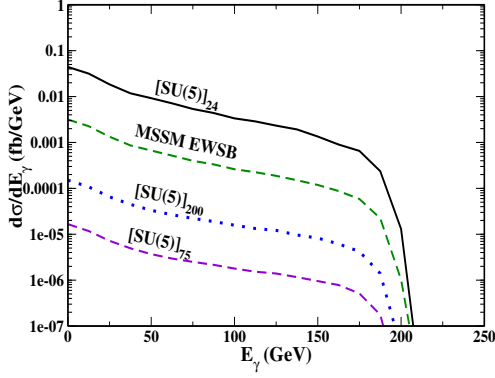


FIG. 10: The photon energy distribution $d\sigma/dE_\gamma$ for the radiative neutralino production including radiative effects for the $SU(5)$ grand unified theory with nonuniversal gaugino masses compared with MSSM EWSB with universal gaugino masses.

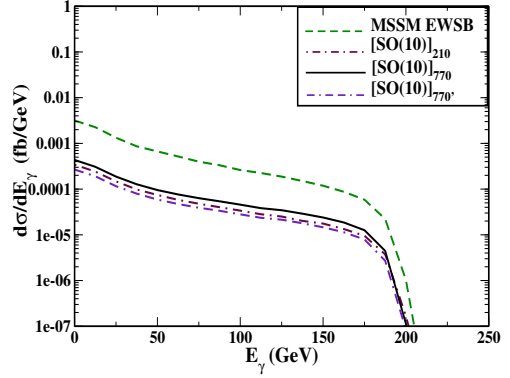


FIG. 11: The photon energy distribution $d\sigma/dE_\gamma$ including radiative effects for the radiative neutralino production for $SO(10)$ grand unified theory with nonuniversal gaugino masses compared with MSSM EWSB with universal gaugino masses.

A. Photon Energy (E_γ) Distribution and Total Beam Energy (\sqrt{s}) Dependence

To begin with, we have calculated the energy distribution of the photons from radiative neutralino production in MSSM EWSB scenario as well as for the different GUT models considered in this paper.

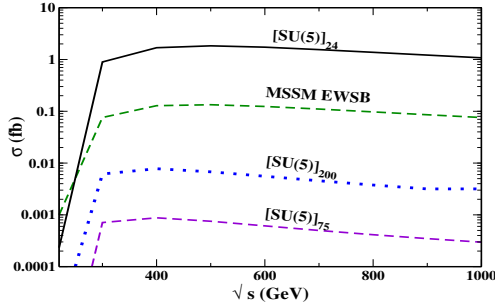


FIG. 12: Total cross section σ for the radiative process $e^+e^- \rightarrow \tilde{\chi}_1^0 \tilde{\chi}_1^0 \gamma$, with the inclusion of radiative effects as a function of center of mass energy \sqrt{s} for the $SU(5)$ grand unified theory with nonuniversal gaugino masses compared with MSSM EWSB scenario with universal gaugino masses at the grand unified scale.

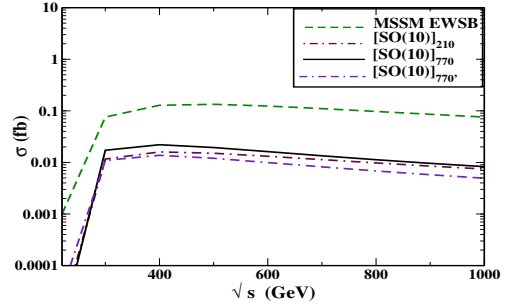


FIG. 13: Total cross section σ for the radiative process $e^+e^- \rightarrow \tilde{\chi}_1^0 \tilde{\chi}_1^0 \gamma$, with the inclusion of radiative effects as a function of center of mass energy \sqrt{s} for the $SO(10)$ grand unified theory with nonuniversal gaugino masses compared with MSSM EWSB scenario with universal gaugino masses at the grand unified scale.

In Table XIII we illustrate the changes in the signal cross section with and without the inclusion of radiative effects for the MSSM EWSB scenario, along with the irreducible SM background with the application of cuts described earlier. The radiative effect leading to the distribution of the beam energy can be distinctly seen from this Table, with the increase of cross section at higher c.m. energies and the corresponding decrease at lower c.m. energies for the signal process. Similar behaviour holds in other models for the signal process and the supersymmetric background processes. In case of the background process, the radiative neutrino production, the presence of the Z pole along with the massless particles in the final state leads to a decrease of cross section at higher c.m. energies and vice versa. The plots here only show the results with the inclusion of radiative effects of ISR and beamstrahlung, since the behaviour in case of different scenarios for the signal process and supersymmetric background with and without the inclusion of radiative effects is similar to the MSSM EWSB scenario shown in Table XIII.

In Figs. 10 and 11 we show the energy distribution of photons for models with nonuniversal gaugino masses

in grand unified theories based on $SU(5)$ and $SO(10)$, where we have included the radiative effects. We have compared this with the photon energy distribution for the MSSM EWSB model with universal gaugino masses at the GUT scale. The energy dependence of the total cross section for these models is also calculated and this is shown in Figs. 12 and 13. From Figs. 10 and 11 as well as from Figs. 12 and 13, it can be seen that the signal in case of MSSM EWSB and $[SU(5)]_{24}$ is enhanced compared to the other scenarios considered here. This is mainly due to the fact that the dominant component of the neutralino in $[SU(5)]_{24}$ is a bino, whereas in other cases the lightest neutralino is dominantly a higgsino state. The MSSM EWSB scenario predicts a lightest neutralino with a dominant higgsino component, but it also has a significant bino component leading to the enhancement of right selectron-electron-neutralino coupling. For the other cases with a higgsino like neutralino the t - and u - channel exchange of $\tilde{e}_{R,L}$, is suppressed, with the only contribution coming from off shell Z decay. In order to find ways of enhancing the signal, one must study the dependence of the signal on selectron $\tilde{e}_{R,L}$ masses as well as on the parameters μ and M_2 , which determine the neutralino mixing elements.

B. Dependence on μ and M_2

As can be seen from the neutralino mass matrix in the Appendix B, the mass of the lightest neutralino depends on the parameters μ and M_2 . Therefore, it is important to study the dependence of cross section of the signal process on these parameters. Since μ and M_2 are independent parameters, we have studied the dependence of the cross section $\sigma(e^+e^- \rightarrow \tilde{\chi}_1^0 \tilde{\chi}_1^0 \gamma)$ on these parameters independently. We have considered here all the scenarios with both universal and nonuniversal gaugino masses. The values of the parameters μ and M_2 are chosen so as to avoid color and charge breaking minima, unbounded from below constraint on scalar potential, and to satisfy phenomenological constraints on different sparticle masses discussed in Appendix B.

We note here that we have carried out a check on the parameter space used in our calculations as to whether the complete scalar potential has charge and color breaking minima (CCB) which is lower than the electroweak minimum. We have also checked whether the scalar potential is unbounded from below (UFB). The criteria used for these conditions are

$$A_f^2 < 3(m_{\tilde{f}_L}^2 + (m_{\tilde{f}_R}^2 + \mu^2 + m_{H_2}), \quad (\text{IV.3})$$

$$m_{H_2} + m_{H_1} \geq 2|B\mu|, \quad (\text{IV.4})$$

respectively, at a scale $Q^2 > M_{\text{EWSB}}^2$. Here f denotes the fermion generation, and A is the trilinear supersymmetry breaking parameter. We have implemented these conditions through the SuSpect package [67] which computes the masses and couplings of the supersymmetric partners of the SM particles. For each model considered in this paper, we perform the renormalization group evolution to calculate the particle spectrum. While doing so we check for the consistency of the chosen parameter set with electroweak symmetry breaking and that the conditions (IV.3) and (IV.4) are satisfied.

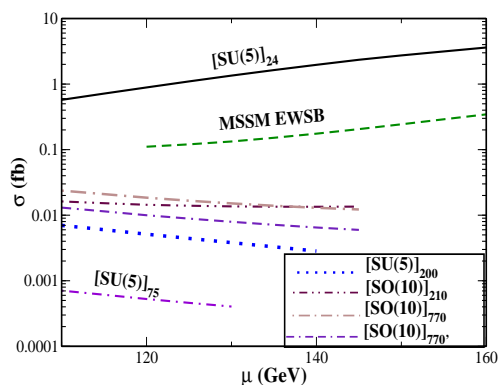


FIG. 14: The total radiative neutralino production cross section σ with radiative effects included as a function of μ in the range $\mu \in [110, 160]$ GeV for different models considered in this paper at $\sqrt{s} = 500$ GeV.

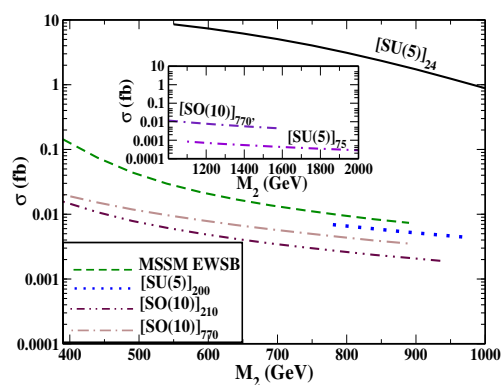


FIG. 15: Total cross section σ with the inclusion of radiative effects for the radiative neutralino production as a function of M_2 for different models with $M_2 \in [390, 1000]$ GeV at $\sqrt{s} = 500$ GeV.

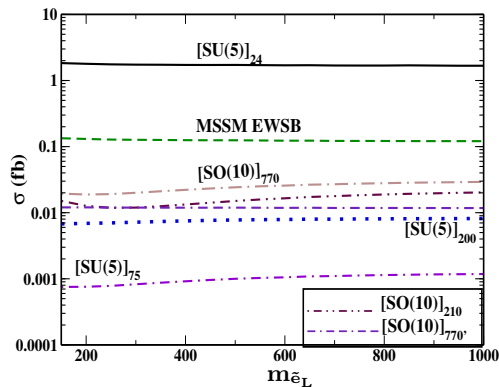


FIG. 16: Total cross section σ for the radiative neutralino production with radiative effects included versus $m_{\tilde{e}_L}$ at $\sqrt{s} = 500$ GeV.

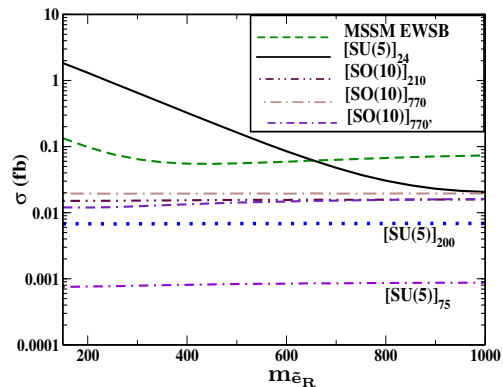


FIG. 17: Total cross section σ along with radiative effects for the radiative neutralino production versus $m_{\tilde{e}_R}$ at $\sqrt{s} = 500$ GeV.

In Fig. 14 we show the μ dependence of the cross section for different models considered in this paper. For a wide range of values of μ , the $[SU(5)]_{24}$ scenario satisfies all experimental constraints, with $\tilde{\chi}_1^0$ as the LSP. Since the neutralino in this case is mainly a bino like state, with values of $\mu > M_1$, the neutralino mass is relatively insensitive to the values of μ . For the other scenarios with a higgsino type lightest neutralino, the cross section is sensitive to the value of μ . Since $m_{\tilde{\chi}_1^0} \propto \mu$, above a certain value of μ , $\tilde{\chi}_1^0$ ceases to be the lightest supersymmetric particle. Depending on the percentage of the higgsino component, the cross section changes with value of μ . In $[SU(5)]_{75}$, since $M_1, M_2 \gg \mu$, $m_{\tilde{\chi}_1^0}$ depends on μ , so from Fig. 14, it can be seen that the signal cross section decreases with μ due to increasing $m_{\tilde{\chi}_1^0}$. Most of the scenarios considered here are tightly constrained as a function of μ , with neutralino as the LSP. This is due to the various limits on the sparticles masses from the experiments. The cross section for some scenarios in this region is too small to be observed at ILC with $\sqrt{s} = 500$ GeV, even with an integrated luminosity of 500 fb^{-1} .

We next show in Fig. 15 the dependence of the radiative neutralino cross section on the soft gaugino mass parameter M_2 for different models that we have studied in this paper. From this Fig. we note that the total cross section decreases with increasing values of M_2 . The elements of the neutralino mixing matrix changes with the variation of the wino parameter M_2 , which in turn change the values of the vertices contributing to the radiative neutralino production, Table XV in the Appendix A. The range of M_2 considered for the different models is taken from Fig. 1. The variation of the cross section with M_2 for $SU(5)_{75}$ and $SO(10)_{770'}$ are shown in the inset of Fig. 15, as their M_2 range is different from the other scenarios. A lower value of M_2 favours a cross section which can be measured experimentally for some scenarios, whereas for higher values the difficulty in measurement of cross section increases.

C. Dependence on selectron masses

The signal process $\sigma(e^+e^- \rightarrow \tilde{\chi}_1^0 \tilde{\chi}_1^0 \gamma)$ mainly proceeds via right and left selectron $\tilde{e}_{R,L}$ exchange in the t - and u -channels. Different models that we have considered in this work have the selectron masses as independent parameters. Figs. 16 and 17 show the dependence of the total cross section σ for the radiative neutralino production on the left and right selectron masses. From Fig. 16 we see that the cross section is not sensitive to the left selectron mass for $[SU(5)]_{24}$ scenario, because the LSP is predominantly a bino. As a consequence, the dominant contribution to the cross section comes from the right selectron exchange, with the contribution from the left selectron exchange suppressed by $\tan \theta_W$ in the coupling, as can be seen from Table XV in the Appendix A. As a consequence the cross section has very little sensitivity to the left selectron mass, but is sensitive to the right selectron mass in the range 150 - 1000 GeV. The MSSM EWSB scenario has a LSP with a dominant contribution coming from higgsino, but has a significant bino contribution as well. Due to this the cross section is relatively insensitive to mass of \tilde{e}_L , but a sensitivity is seen with respect to right selectron mass.

In the other scenarios with a higgsino type LSP, the neutralino coupling with $\tilde{e}_{R,L}$ is suppressed, making these almost insensitive to the selectron masses. As can be seen from the Figs. 16 and 17, the cross section for these scenarios has very little sensitivity to the left and right selectron mass. The suppressed couplings lead to a reduction in the cross section.

V. BACKGROUND PROCESSES

A. The Neutrino Background

The SM radiative neutrino production is the main irreducible background for the process radiative neutralino production (III.1). The other possible backgrounds are from $e^+e^- \rightarrow \tau^+\tau^-\gamma$, with both the τ 's decaying to soft leptons or hadrons but the contribution from this process is found to be negligible. Another large background is from the radiative Bhabha scattering, $e^+e^- \rightarrow e^+e^-\gamma$, where e^\pm 's are not detected. This radiative scattering is usually eliminated by imposing a cut on E_γ . The events are selected by imposing the condition that any particle other than γ appearing in the angular range $-0.95 < \cos\theta_\gamma < 0.95$ must have energy less than E_{max} , where E_{max} is detector dependent, but presumably no larger than a few GeV. This is discussed in detail in the literature [68].

The SM radiative neutrino production

$$e^+ + e^- \rightarrow \nu_\ell + \bar{\nu}_\ell + \gamma, \quad \ell = e, \mu, \tau, \quad (\text{V.1})$$

has been studied extensively [43, 50, 69–71]. For this background process ν_e are produced via t -channel W boson exchange, and $\nu_{e,\mu,\tau}$ via s -channel Z boson exchange. The corresponding Feynman diagrams are shown in Fig. 18.

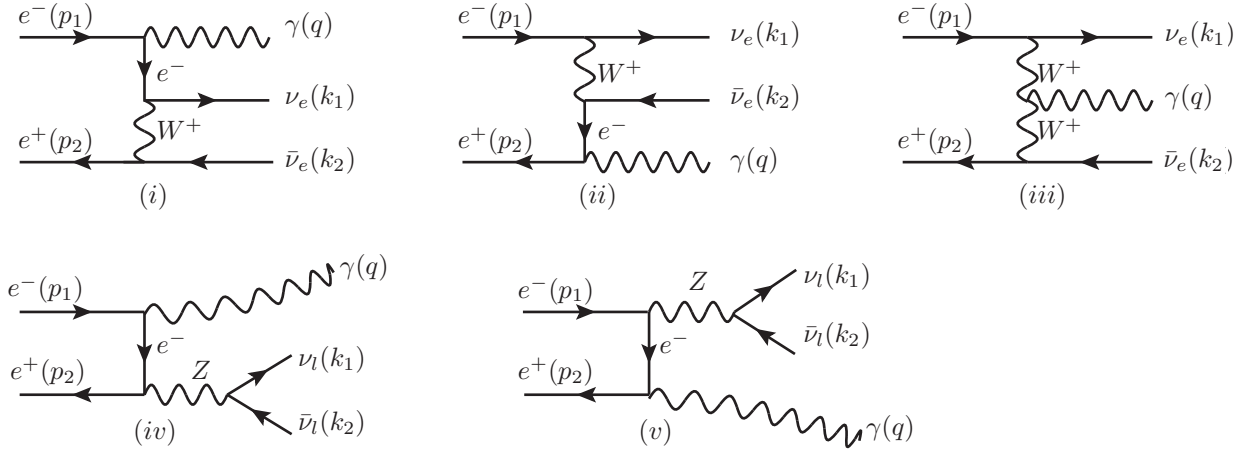


FIG. 18: Feynman diagrams contributing to the radiative neutrino process $e^+e^- \rightarrow \nu\bar{\nu}\gamma$ where (iv and v) corresponds to the neutrinos of three flavours

The background photons from this process tend to be mostly in the forward and backward directions as compared to the signal photons, therefore the detector acceptance cut for the photon is applied as $|\cos\theta_\gamma| < 0.95$. This SM background has the same photon energy distribution $d\sigma/dE_\gamma$ and the \sqrt{s} dependence of the cross section σ for all the scenarios studied in this paper. Fig. 19 shows that the photon energy distribution from the radiative neutrino production peaks at $E_\gamma = (s - m_{Z^0}^2)/(2\sqrt{s}) \approx 244$ GeV because of the radiative Z^0 production ($\sqrt{s} > m_{Z^0}$). The result is presented here with and without the higher order QED radiative effects. The inclusion of radiative effects make the peak due to the radiative return of Z^0 slightly broad. By imposing an upper cut on the photon energy $x^{\max} = E_\gamma^{\max}/E_{\text{beam}} = 1 - m_{\chi_1^0}^2/E_{\text{beam}}^2$, see Eq. (IV.1), the photon background from radiative neutrino production can be reduced, by elimination of the on-shell Z^0 contribution to the background cross section. From the Feynman diagrams for the background process, Fig. 18, it can be seen that this process has a strong polarization dependence on the initial beams due to the exchange of W bosons which couples only to left handed electron and right handed positron. Therefore, with a suitable choice of beam polarization along with various kinematical cuts discussed earlier, the contribution from the background process can be significantly reduced.

In Fig. 20 we show the \sqrt{s} dependence of the total radiative neutrino cross section, with and without the inclusion of higher order QED radiative effects. Without the upper cut on the photon energy x^{\max} , the background cross section from radiative neutrino production $e^+e^- \rightarrow \nu\bar{\nu}\gamma$ is much larger than the corresponding cross section with the cut, near the Z^0 production threshold. The main purpose of the cut is to move away from the Z^0 peak. When we impose the cut, the signal cross section from radiative neutralino production is

approximately three orders of magnitude smaller than the background in the case of MSSM EWSB and the various GUT models.

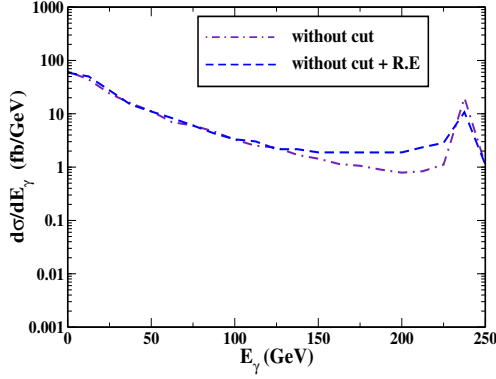


FIG. 19: Plot showing the photon energy distribution $d\sigma/dE_\gamma$ for the radiative neutrino production process $e^+e^- \rightarrow \nu\bar{\nu}\gamma$ at $\sqrt{s} = 500$ GeV, with and without including radiative effects (R.E.).

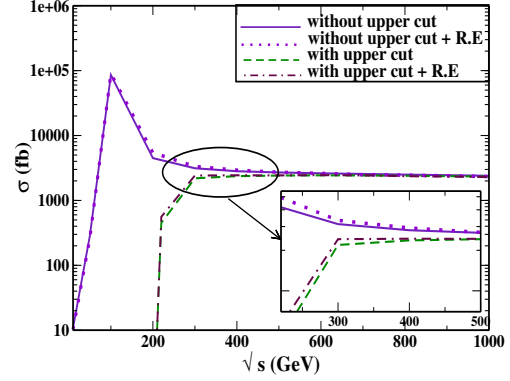


FIG. 20: The total energy \sqrt{s} dependence of the radiative neutrino cross section with and without an upper cut on the photon energy E_γ , along with and without the consideration of radiative effects (R.E.).

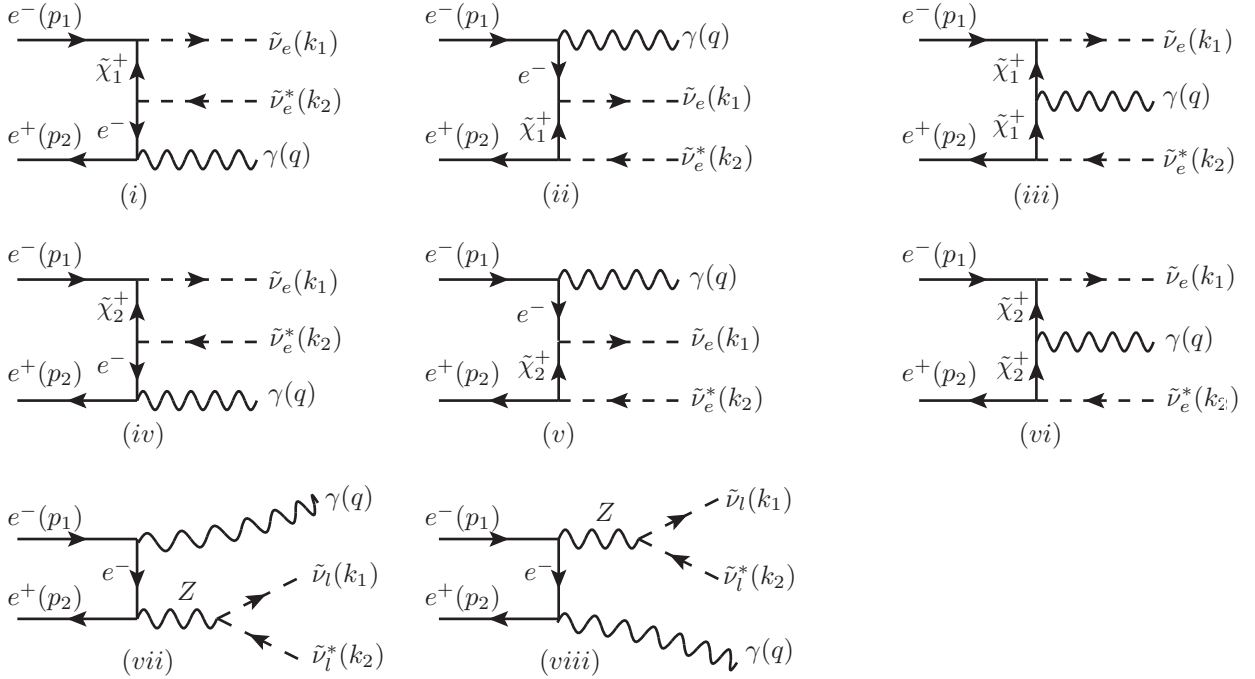


FIG. 21: Feynman diagrams contributing to the radiative sneutrino production process $e^+e^- \rightarrow \tilde{\nu}\tilde{\nu}^*\gamma$, with the last two diagrams (vii and viii) corresponding to all the leptonic sneutrino

B. The Supersymmetric Background

The radiative neutralino production (III.1) has also a supersymmetric background coming from the sneutrino production process [43, 72]

$$e^+ + e^- \rightarrow \tilde{\nu}_\ell + \tilde{\nu}_\ell^* + \gamma, \quad \ell = e, \mu, \tau. \quad (\text{V.2})$$

This is in addition to the background from the SM process (V.1). The lowest order Feynman diagrams contributing to the process (V.2) are shown in Fig. 21. This background process receives t -channel contributions via virtual charginos for $\tilde{\nu}_e \tilde{\nu}_e^*$ production, as well as s -channel contributions from Z boson exchange for $\tilde{\nu}_{e,\mu,\tau} \tilde{\nu}_{e,\mu,\tau}^*$ production. In Fig. 22 we show the photon energy distribution $d\sigma/dE_\gamma$ for radiative sneutrino production $e^+e^- \rightarrow \tilde{\nu} \tilde{\nu}^* \gamma$ at $\sqrt{s} = 500$ GeV for the MSSM EWSB and grand unified scenarios. The total cross section for the radiative sneutrino production is shown in Fig. 23. Since $\tilde{\nu}_e \tilde{\nu}_e^*$ production receives t -channel contributions via virtual charginos, the production cross section as well as the photon energy distribution depends on the chargino mixing matrix \mathbf{U} for the different scenarios. The cuts applied to this process are the same as discussed before.

As can be seen from Fig. 23 radiative sneutrino production (V.2) can be a major supersymmetric background to neutralino production (III.1) if sneutrinos decay invisibly, e.g. via $\tilde{\nu} \rightarrow \tilde{\chi}_1^0 \nu$. This scenario has been called “virtual LSP” scenario [43]. However, if kinematically allowed, other visible decay channels like $\tilde{\nu} \rightarrow \tilde{\chi}_1^\pm \ell^\mp$ reduce the background rate from radiative sneutrino production. In the scenarios with a bino type neutralino, as in $[SU(5)]_{24}$, the branching ratio $\text{BR}(\tilde{\nu}_e \rightarrow \tilde{\chi}_1^0 \nu_e) = 100\%$, and, therefore, this process serves as a dominant background. However, for the other cases where higgsino is the dominant component we have the branching ratios as given in Table XIV. The second lightest neutralino being heavier than the sneutrino $\tilde{\nu}_e$ in MSSM EWSB scenario, the branching ratio is kinematically not accessible.

Branching Ratios	MSSM EWSB	$SU(5)_{75}$	$SU(5)_{200}$	$SO(10)_{210}$	$SO(10)_{770}$	$SO(10)_{770'}$
$\text{BR}(\tilde{\nu}_e \rightarrow \tilde{\chi}_1^0 \nu_e)$	78.4%	8.1%	21.2%	18%	24.2%	44.4%
$\text{BR}(\tilde{\nu}_e \rightarrow \tilde{\chi}_2^0 \nu_e)$		1.8%	4.54%	0.8%	1.2%	6%
$\text{BR}(\tilde{\nu} \rightarrow \tilde{\chi}_1^\pm \ell^\mp)$	21.6%	90.1%	74.3%	81%	74.8%	49.6%

TABLE XIV: Branching ratios of the sneutrino for different models with a higgsino type lightest neutralino

Furthermore, neutralino production $e^+e^- \rightarrow \tilde{\chi}_1^0 \tilde{\chi}_2^0$ followed by subsequent radiative neutralino decay [73] $\tilde{\chi}_2^0 \rightarrow \tilde{\chi}_1^0 \gamma$ is also a potential background. However, significant branching ratios $\text{BR}(\tilde{\chi}_2^0 \rightarrow \tilde{\chi}_1^0 \gamma) > 10\%$ are only obtained for small values of $\tan\beta < 5$ or $M_1 \sim M_2$ [44, 74, 75]. Thus, we neglect this background, detailed discussions of which can be found in Refs. [74–76].

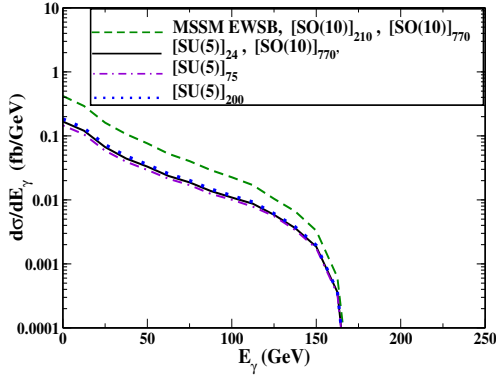


FIG. 22: Plot showing the photon energy distribution $d\sigma/dE_\gamma$ for the radiative sneutrino production process $e^+e^- \rightarrow \tilde{\nu} \tilde{\nu}^* \gamma$ at $\sqrt{s} = 500$ GeV, with the inclusion of radiative effects.

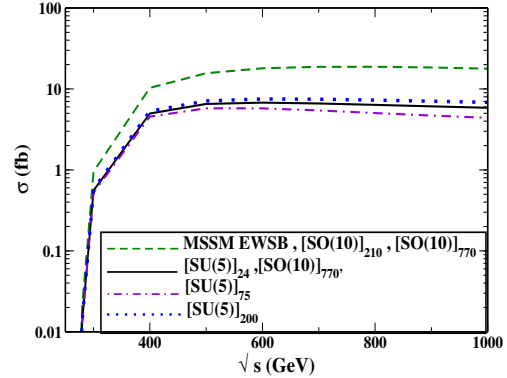


FIG. 23: The total energy \sqrt{s} dependence of the radiative sneutrino cross section $e^+e^- \rightarrow \tilde{\nu} \tilde{\nu}^* \gamma$ with an upper cut on the photon energy E_γ and the inclusion of radiative effects.

C. Theoretical Significance

Finally we address the issue of whether the photons coming from the signal process can be measured over the photons coming from the background SM process. The excess of signal photons $N_S = \sigma \mathcal{L}$ over the SM background photons $N_B = \sigma_B \mathcal{L}$ for a given integrated luminosity \mathcal{L} can be expressed in terms of the theoretical significance [66]

$$S = \frac{N_S}{\sqrt{N_S + N_B}} = \frac{\sigma}{\sqrt{\sigma + \sigma_B}} \sqrt{\mathcal{L}}. \quad (\text{V.3})$$

A theoretical significance of $S = 1$ means that the signal can be measured at a 68 % confidence level, whereas one needs a significance of 5 for the detection of the signal. Both the signal and the background process depends significantly on the beam energy for $\sqrt{s} = 500$ GeV and $\mathcal{L} = 5 \times 10^2 \text{ fb}^{-1}$. In Fig. 24 we show the μ dependence of the theoretical significance S for the different models considered here. When the lightest neutralino is dominantly a bino type state, then for μ in the range $\mu \in [120, 160]$ GeV, the significance can be a maximum of about 2, for the given luminosity. Then the signal for the radiative neutralino production would be seen at ILC as shown in Fig. 24. But for the scenarios with the higgsino as the dominant component of the lightest neutralino, it will be difficult to observe the signal.

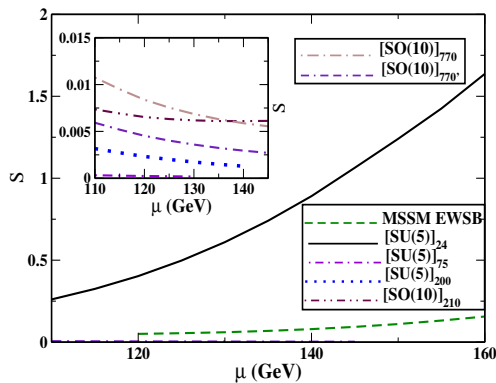


FIG. 24: Plot showing the theoretical significance S for the radiative neutralino production as a function of μ for different models considered in this paper with $\sqrt{s} = 500$ GeV.

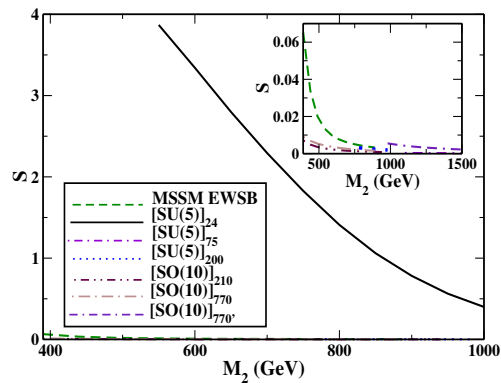


FIG. 25: The theoretical significance S for the radiative neutralino production as a function of the gaugino mass parameter M_2 for the different models with $\sqrt{s} = 500$ GeV.

We have also studied the variation of theoretical significance S as a function of the gaugino mass parameter M_2 as well. The M_2 dependence of S for all the models considered in this paper is shown in Fig. 25 in the interval $M_2 \in [200, 1000]$ GeV. The behaviour is similar to μ with the models having a relatively higher value of S for lower value of M_2 . The values of S given here can be considered as a good guideline, since we do not include a detector simulation here. Besides the theoretical significance, one must also consider the signal to background ratio N_S/N_B in order to judge the reliability of the analysis. Overall the process under study for the different scenarios considered here, specially the one with a higgsino type neutralino, will most probably not be useful for extending the SUSY parameter space reach of ILC. However, it may be possible to reduce the SM background if the electron and positron beams are polarized, with right handed electrons and left handed positrons.

The theoretical significance for most of the scenarios thus considered is too small, making it difficult to test them in the future linear colliders through the radiative neutralino production. But these scenarios have a distinctive feature which make it possible to test them, by means of a hard photon tag as employed for the process (I.1).

For some of the scenarios considered here, namely $[SU(5)]_{75}$, $[SU(5)]_{200}$, $[SO(10)]_{210}$ and $[SO(10)]_{770'}$, due to large values of $M_{1,2}$ and a low value of μ , the states $\tilde{\chi}_1^0, \tilde{\chi}_2^0$ and $\tilde{\chi}_1^\pm$ are nearly degenerate, with mass around μ , and all of them having dominant higgsino component. Since they are all closely degenerate in mass, with $m_{\tilde{\chi}_2^0} - m_{\tilde{\chi}_1^0}$ around 15 GeV, therefore the processes (a) $e^+e^- \rightarrow \tilde{\chi}_1^0 \tilde{\chi}_2^0 \gamma$ and (b) $e^+e^- \rightarrow \tilde{\chi}_2^0 \tilde{\chi}_2^0 \gamma$ will also act as supersymmetric background to the radiative neutralino production. The radiative sneutrino production in

these scenarios with a higgsino like LSP has visible decay channels, and can, therefore, be easily discriminated. Since the $Z\tilde{\chi}_1^0\tilde{\chi}_2^0$ coupling is much larger as compared to $Z\tilde{\chi}_1^0\tilde{\chi}_1^0$ coupling, therefore a detailed study of the signatures with a hard photon and large missing energy in the final state will include processes (a), (b) and the radiative neutralino production. If investigated through the above channel the signal for these scenarios will be comparable to the SM irreducible background, in contrast to the case when only the process (I.1) is considered. We show in Figs. 26 and 27 the photon energy distribution and the cross section for these models for different cases as follows:

- Case 1:
Selecting events with $\gamma +$ missing energy in the final state, which includes the process (a), (b) and the radiative neutralino production.
- Case 2:
The contribution from SM irreducible background, the radiative neutrino production.
- For comparison we have also shown the case of radiative neutralino production $\tilde{\chi}_1^0\tilde{\chi}_1^0\gamma$ in these Figs.

The radiative effects are included in all these calculations. It can be seen from these Figs. that the selection of events with $\gamma +$ missing energy in the final state gives almost the same distribution and cross section for all the models considered. The models can not be discriminated but their signature is strong compared to the previous analyses in subsection. IV A. The theoretical significance in this mode at $\sqrt{s} = 500$ GeV, increases to about 22, compared to 0.001 for $[SU(5)]_{75}$, for the parameter values given in Table IV. Similar result holds for the other scenarios.

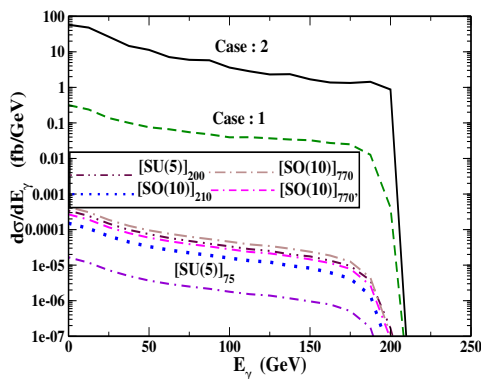


FIG. 26: The photon energy distribution $\frac{d\sigma}{dE_\gamma}$ including radiative effects for different cases at $\sqrt{s} = 500$ GeV

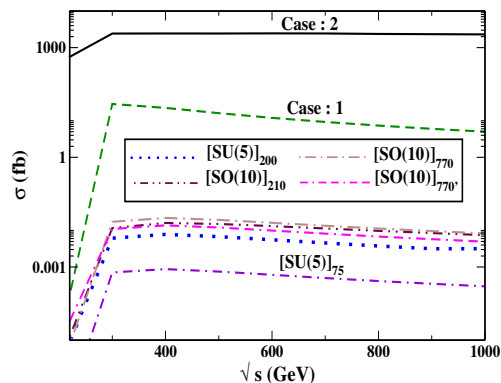


FIG. 27: The total energy \sqrt{s} dependence for the different cases defined in the text with the inclusion of radiative effects.

VI. SUMMARY AND CONCLUSIONS

We have carried out a detailed analysis of the radiative neutralino production $e^+e^- \rightarrow \tilde{\chi}_1^0\tilde{\chi}_1^0\gamma$ in various GUT models for the International Linear Collider energies and compared it with the corresponding results in the MSSM with universal gaugino mass parameters. In these models the boundary conditions on the soft gaugino mass parameters can be nonuniversal and hence different from those of MSSM with universal boundary conditions. This process has a signature of a high energy photon and missing energy. We have obtained a typical set of parameter values by excluding certain regions of the parameter space which follow from theoretical and experimental constraints, as discussed in Appendix. B.

Using this parameter set, we have studied in detail the signal cross section for the ILC energies with unpolarized e^+ and e^- beams. For comparison, we have used the MSSM EWSB scenario as a benchmark. The contributions from the SM background $e^+e^- \rightarrow \nu\bar{\nu}\gamma$, as well as the supersymmetric process $e^+e^- \rightarrow \tilde{\nu}\tilde{\nu}^*\gamma$ acting as a background to the radiative neutralino production are also considered. All these processes have a signature of a highly energetic photon with missing energy. The photon energy distribution $d\sigma/dE_\gamma$, and the total cross section as a function of the total centre of mass energy have been calculated for MSSM EWSB, as

well as for the different scenarios considered here, at $\sqrt{s} = 500$ GeV using the programme CalcHEP. Since ISR and beamstrahlung are a part of the future linear colliders, due to the planned high luminosity, for a realistic prediction we have also included these radiative effects. The dependence of the cross section for radiative neutralino production on the $SU(2)_L$ gaugino mass parameter M_2 and the Higgs(ino) mass parameter μ , as well as its dependence on the selectron (\tilde{e}_R, \tilde{e}_L) masses has also been studied and compared with the corresponding results in MSSM EWSB. We have considered scenarios based on $SU(5)$ and $SO(10)$ grand unified theories with nonuniversal gaugino mass at the grand unified scale. In the case of $SU(5)$ and $SO(10)$ models we evolve the parameters to the electroweak scale and then use these to evaluate the radiative neutralino cross section. All the results mainly depend on the composition of the lightest neutralino in the different models considered here. The models with bino as a dominant component of the lightest neutralino behave differently from the models with higgsino as the dominant component of the lightest neutralino. The composition of the lightest neutralino depends on the ratio of the soft gaugino mass parameters at the electroweak scale and μ . The values for these parameters are chosen satisfying all the experimental constraints, along with the requirement that the lightest neutralino is the LSP. The supersymmetric background coming from the radiative sneutrino production is also calculated which depends on the chargino mixing matrix. The dependence of cross section for these two distinct scenarios is valid for different ranges of the parameters M_2 and μ . Finally, in order to understand whether an excess of signal photons, N_S , can be measured over the background photons, N_B , from radiative neutrino production, we have analysed the theoretical statistical significance $S = N_S/\sqrt{N_S + N_B}$, and studied its dependence on the independent parameters M_2 and μ , that enter the neutralino mass matrix. It is seen that the signal for some scenarios is too weak to be seen at ILC. Therefore for some of these scenarios which also predict the second lightest neutralino to be degenerate with the LSP, the observance of a signature of a highly energetic photon with missing energy taking into account the second lightest neutralino production along with LSP production is also considered. We have also noted that initial beam polarization may reduce the background, and it may be interesting to study whether the signal for radiative neutralino production can be enhanced by using polarized beams. This question in the context of the GUT models will be studied in a separate paper [77].

VII. ACKNOWLEDGEMENTS

The authors would like to thank B. Ananthanarayan for many useful discussions. P. N. P. would like to thank the Centre for High Energy Physics, Indian Institute of Science, Bangalore for hospitality while this work was initiated. The work of P. N. P. is supported by the J. C. Bose National Fellowship of the Department of Science and Technology, and by the Council of Scientific and Industrial Research, India under the project No. (03)(1220)/12/EMR-II. P. N. P would like to thank the Inter-University Centre for Astronomy and Astrophysics, Pune, India for hospitality where part of this work carried out.

Appendix A: Neutralino Mass Matrix, Lagrangian and Couplings

In this Appendix we summarize the mixing matrix for the neutralinos, and the couplings that enter our calculations. We recall that the neutralino mass matrix receives contribution from MSSM superpotential term

$$W_{\text{MSSM}} = \mu H_1 H_2, \quad (\text{A.1})$$

where H_1 and H_2 are the Higgs doublet chiral superfields with opposite hypercharge, and μ is the supersymmetric Higgs(ino) parameter. In addition to (A.1), the neutralino mass matrix receives contributions from the interactions between gauge and matter multiplets, as well as contributions from the soft supersymmetry breaking masses for the $SU(2)_L$ and $U(1)_Y$ gauginos. Putting together all these contributions, the neutralino mass matrix, in the bino, wino, higgsino basis ($-i\lambda', -i\lambda^3, \psi_{H_1}^1, \psi_{H_2}^2$) can be written as [4, 51]

$$M_{\text{MSSM}} = \begin{pmatrix} M_1 & 0 & -m_Z \sin \theta_W \cos \beta & m_Z \sin \theta_W \sin \beta \\ 0 & M_2 & m_Z \cos \theta_W \cos \beta & -m_Z \cos \theta_W \sin \beta \\ -m_Z \sin \theta_W \cos \beta & m_Z \cos \theta_W \cos \beta & 0 & -\mu \\ m_Z \sin \theta_W \sin \beta & -m_Z \cos \theta_W \sin \beta & -\mu & 0 \end{pmatrix}, \quad (\text{A.2})$$

where M_1 and M_2 are the $U(1)_Y$ and the $SU(2)_L$ soft supersymmetry breaking gaugino mass parameters, respectively, and $\tan \beta = v_2/v_1$ is the ratio of the vacuum expectation values of the neutral components of the two Higgs doublet fields H_1 and H_2 , respectively. Furthermore, m_Z is the Z boson mass, and θ_W is the weak mixing angle. We shall consider all parameters in the neutralino mass matrix to be real. In this case it can

be diagonalised by an orthogonal matrix. If one of the eigenvalues of M_{MSSM} is negative, one can diagonalize this matrix using a unitary matrix N , the neutralino mixing matrix, to get a positive semi definite diagonal matrix [51] with the neutralino masses $m_{\tilde{\chi}_i^0}$ ($i = 1, 2, 3, 4$) in order of increasing value:

$$N^* M_{\text{MSSM}} N^{-1} = \text{diag} (m_{\tilde{\chi}_1^0}, m_{\tilde{\chi}_2^0}, m_{\tilde{\chi}_3^0}, m_{\tilde{\chi}_4^0}). \quad (\text{A.3})$$

For the minimal supersymmetric standard model the interaction Lagrangian of neutralinos, electrons, selectrons and Z bosons is given by [51]

$$\begin{aligned} \mathcal{L} = & \left(-\frac{\sqrt{2}e}{\cos \theta_W} N_{11}^* \bar{f}_e P_L \tilde{\chi}_1^0 \tilde{e}_R + \frac{e}{\sqrt{2} \sin \theta_W} (N_{12} + \tan \theta_W N_{11}) \bar{f}_e P_R \tilde{\chi}_1^0 \tilde{e}_L \right. \\ & + \frac{e}{4 \sin \theta_W \cos \theta_W} (|N_{13}|^2 - |N_{14}|^2) Z_\mu \tilde{\chi}_1^0 \gamma^\mu \gamma^5 \tilde{\chi}_1^0 \\ & \left. + e Z_\mu \bar{f}_e \gamma^\mu \left[\frac{1}{\sin \theta_W \cos \theta_W} \left(\frac{1}{2} - \sin^2 \theta_W \right) P_L - \tan \theta_W P_R \right] f_e + \text{h.c.}, \right. \end{aligned} \quad (\text{A.4})$$

with the electron, selectrons, neutralino and Z boson fields denoted by f_e , $\tilde{e}_{L,R}$, $\tilde{\chi}_1^0$, and Z_μ , respectively, and $P_{R,L} = \frac{1}{2} (1 \pm \gamma^5)$. The interaction vertices following from (A.4) are summarized in Table XV.

TABLE XV: Vertices corresponding to different terms in the interaction Lagrangian (A.4) for MSSM. Here we have also shown the vertices for selectron-photon and electron-photon interactions [17].

Vertex	Vertex Factor
right selectron - electron - neutralino	$\frac{-ie\sqrt{2}}{\cos \theta_W} N_{11}^* P_L$
left selectron - electron - neutralino	$\frac{ie}{\sqrt{2} \sin \theta_W} (N_{12} + \tan \theta_W N_{11}) P_R$
neutralino - Z^0 - neutralino	$\frac{ie}{4 \sin \theta_W \cos \theta_W} (N_{13} ^2 - N_{14} ^2) \gamma^\mu \gamma^5$
electron - Z^0 - electron	$ie \gamma^\mu \left[\frac{1}{\sin \theta_W \cos \theta_W} \left(\frac{1}{2} - \sin^2 \theta_W \right) P_L - \tan \theta_W P_R \right]$
selectron - photon - selectron	$ie(p_1 + p_2)^\mu$
electron - photon - electron	$ie \gamma^\mu$

Appendix B: Experimental Constraints

In this Appendix we review the constraints on the SUSY particle spectrum from the different experiments at LHC, Tevatron and LEP.

1. Limits on Gaugino mass parameters

The exclusion limit on the gaugino mass parameters is set from the current experimental limits on the superpartner masses. Since no supersymmetric partners of the SM particles have been detected in the experiments, only lower limits on their masses have been obtained. In particular, the search for the lightest chargino state at LEP has yielded lower limits on its mass [52]. The lower limit depends on the spectrum of the model [53]. Assuming that m_0 , the soft supersymmetry breaking scalar mass, is large, the limit on the lightest chargino mass following from non observation of chargino pair production in e^+e^- collisions is

$$M_{\tilde{\chi}_1^\pm} \gtrsim 103 \text{ GeV}. \quad (\text{B.1})$$

The limit depends on the sneutrino mass. For a sneutrino mass below 200 GeV, the bound becomes weaker, since the production of a chargino pair becomes more rare due to the destructive interference between γ or Z in the s -channel and $\tilde{\nu}$ in the t -channel. In the models we consider, $m_{\tilde{\nu}}$ is close to m_0 . When $m_{\tilde{\nu}} < 200$ GeV, but $m_{\tilde{\nu}} > m_{\tilde{\chi}^\pm}$, the limit becomes [53]

$$M_{\tilde{\chi}^\pm} \gtrsim 85 \text{ GeV}. \quad (\text{B.2})$$

For the parameters of the chargino mass matrix, the limit (B.1) implies an approximate lower limit [54, 55]

$$M_2, \mu \gtrsim 100 \text{ GeV}. \quad (\text{B.3})$$

The limits shown in Eq. (B.3) on M_2 and μ are obtained by scanning over the MSSM parameter space and are, therefore, expected to be model independent [12]. From the chargino mass limit from LEP, a neutralino mass limit is obtained assuming gaugino mass unification at high energy scales and amounts to 47 GeV. But due to the strong constraints from LHC experiments, the lower limit on $\tilde{\chi}_1^0$ in case of constrained MSSM (CMSSM) has risen to about 100 GeV.

2. Exclusion limits on squarks and gluinos

Experiments at the LHC and Tevatron being the proton-(anti) proton collider, with their higher centre of mass energies compared to LEP, is more sensitive for the SUSY particles carrying color charge, squarks and gluinos, because of QCD-mediated processes. Limits of the order of about 100 GeV, was set on the squark masses by LEP, but the recent hadron collider experiments have set much higher limits.

Gluino masses below 800 GeV, are excluded by both ATLAS and CMS collaboration in the framework of CMSSM for all squark masses. For equal squark and gluino masses, the limit is around 1400 GeV [78, 79]. These results are only slightly dependent on the choice of the CMSSM parameters, $\tan\beta$, A_0 and μ . Similar analyses has been carried out in the context of simplified models, where upper limits on gluino pair production are derived as a function of the gluino and the lightest neutralino mass. For massless LSP, $m_{\tilde{g}} < 900$ GeV is excluded. For a heavy LSP above 300 GeV, no general limit on gluino can be set.

Limits on the first two generation squark masses are set by the LHC experiments, with lowers limits of around 1300 GeV [78, 79], for all gluino masses in the framework of CMSSM. The analyses for squarks are similar to the gluinos. For massless neutralino in the framework of simplified models, squark masses below 750 GeV are excluded, whereas increasing the mass of LSP above 200 GeV leads to a degradation of the limits.

The limits on the third generation \tilde{t}_1 mass from LEP was around 96 GeV, in the charm plus neutralino final state [52]. LHC along with Tevatron have performed the analyses for third generation squarks in different scenarios, leading to different final states [80]. Similar analyses has been carried out for the sbottom quarks. Overall, for our analyses we are considering the scenario where the third generation squarks are excluded below a mass of about 800 GeV.

3. Exclusion limit on slepton masses

The strongest limit on the slepton masses come from LEP, because of its clean signature. LEP experiments [52] have excluded sleptons for masses below 100 GeV in case of different scenarios. Similarly for the sneutrinos, limits are obtained from the invisible width of the Z boson along with the limits derived from the searches of gauginos and sleptons. They are excluded for a mass of about 94 GeV.

Taking into account all the above constraints set by the LEP and LHC experiments, for our analyses we have taken $m_{\tilde{g}} \approx 1400$ GeV, mass of first two generation squarks around 1300 GeV, $m_{\tilde{t}}$ around 1000 GeV along with the slepton masses around 150 GeV.

-
- [1] J. Wess and J. Bagger, "Supersymmetry and supergravity," *Princeton, USA: Univ. Pr. (1992)* 259 p
 - [2] G. 't Hooft, C. Itzykson, A. Jaffe, H. Lehmann, P. K. Mitter, I. M. Singer and R. Stora, NATO Adv. Study Inst. Ser. B Phys. **59**, 1 (1980); E. Witten, Nucl. Phys. B **188**, 513 (1981); R. K. Kaul, Phys. Lett. B **109**, 19 (1982); R. K. Kaul and P. Majumdar, Nucl. Phys. B **199**, 36 (1982); R. K. Kaul, Pramana **19**, 183 (1982).
 - [3] H. P. Nilles, Phys. Rept. **110**, 1 (1984); P. Nath, R. L. Arnowitt and A. H. Chamseddine, NUB-2613.

- [4] A. Bartl, H. Fraas, W. Majerotto and N. Oshimo, Phys. Rev. D **40**, 1594 (1989).
- [5] A. Bartl, H. Fraas and W. Majerotto, Nucl. Phys. B **278**, 1 (1986).
- [6] P. N. Pandita, Phys. Rev. D **50**, 571 (1994).
- [7] P. N. Pandita, Z. Phys. C **63**, 659 (1994).
- [8] P. N. Pandita, Phys. Rev. D **53**, 566 (1996).
- [9] P. N. Pandita, arXiv:hep-ph/9701411.
- [10] S. Y. Choi, J. Kalinowski, G. A. Moortgat-Pick and P. M. Zerwas, Eur. Phys. J. C **22**, 563 (2001) [Addendum-ibid. C **23**, 769 (2002)] [arXiv:hep-ph/0108117].
- [11] K. Huitu, J. Laamanen and P. N. Pandita, Phys. Rev. D **67**, 115009 (2003) [arXiv:hep-ph/0303262].
- [12] K. Huitu, J. Laamanen, P. N. Pandita and P. Tiitola, Phys. Rev. D **82**, 115003 (2010) [arXiv:1006.0661 [hep-ph]].
- [13] S. Dimopoulos, S. Raby and F. Wilczek, Phys. Rev. D **24**, 1681 (1981).
- [14] P. Langacker and N. Polonsky, Phys. Rev. D **52**, 3081 (1995) [arXiv:hep-ph/9503214]; U. Amaldi, W. de Boer and H. Furstenau, Phys. Lett. B **260**, 447 (1991); C. Giunti, C. W. Kim and U. W. Lee, Mod. Phys. Lett. A **6**, 1745 (1991).
- [15] G. Altarelli, F. Feruglio and I. Masina, JHEP **0011**, 040 (2000) [arXiv:hep-ph/0007254].
- [16] G. Altarelli and F. Feruglio, New J. Phys. **6**, 106 (2004) [arXiv:hep-ph/0405048].
- [17] For a review and references, see e.g. R. Basu, P. N. Pandita and C. Sharma, Phys. Rev. D **77**, 115009 (2008) [arXiv:0711.2121 [hep-ph]].
- [18] E. Cremmer, S. Ferrara, L. Girardello and A. Van Proeyen, Phys. Lett. B **116**, 231 (1982).
- [19] L. Randall and R. Sundrum, Nucl. Phys. B **557**, 79 (1999) [arXiv:hep-th/9810155]; G. F. Giudice, M. A. Luty, H. Murayama and R. Rattazzi, JHEP **9812**, 027 (1998) [arXiv:hep-ph/9810442].
- [20] K. Huitu, J. Laamanen and P. N. Pandita, Phys. Rev. D **65**, 115003 (2002) [hep-ph/0203186].
- [21] J. R. Ellis, K. Enqvist, D. V. Nanopoulos and K. Tamvakis, Phys. Lett. B **155**, 381 (1985); M. Drees, Phys. Lett. B **158**, 409 (1985). G. Anderson, C. H. Chen, J. F. Gunion, J. D. Lykken, T. Moroi and Y. Yamada, *In the Proceedings of 1996 DPF / DPB Summer Study on New Directions for High-Energy Physics (Snowmass 96), Snowmass, Colorado, 25 Jun - 12 Jul 1996, pp SUP107* [arXiv:hep-ph/9609457].
- [22] V.D. Barger and C. Kao, Phys. Rev. **D60**, 115015 (1999); G. Anderson, H. Baer, C.-H. Chen, and X. Tata, Phys. Rev. **D61**, 095005 (2000).
- [23] K. Huitu, Y. Kawamura, T. Kobayashi, and K. Puolamäki, Phys. Rev. **D61**, 035001 (2000); G. Bélanger, F. Boudjema, A. Cottrant, A. Pukhov and A. Semenov, Nucl. Phys. **B706**, 411 (2005).
- [24] A. Djouadi, Y. Mambrini and M. Muhlleitner, Eur. Phys. J. C **20**, 563 (2001) [arXiv:hep-ph/0104115].
- [25] V. Bertin, E. Nezri, and J. Orloff, JHEP **0302**, 046 (2003); A. Birkedal-Hansen and B.D. Nelson, Phys. Rev. **D67**, 095006 (2003); U. Chattopadhyay and D.P. Roy, Phys. Rev. **D68**, 033010 (2003).
- [26] A. Corsetti and P. Nath, Phys. Rev. **D64**, 125010 (2001).
- [27] J. A. Aguilar-Saavedra *et al.* [ECFA/DESY LC Physics Working Group], “TESLA Technical Design Report Part III: Physics at an e+e- Linear Collider,” arXiv:hep-ph/0106315.
- [28] T. Abe *et al.* [American Linear Collider Working Group], “Linear collider physics resource book for Snowmass 2001. 1: Introduction,” in *Proc. of the APS/DPF/DPB Summer Study on the Future of Particle Physics (Snowmass 2001)* ed. N. Graf, arXiv:hep-ex/0106055.
- [29] K. Abe *et al.* [ACFA Linear Collider Working Group], “Particle physics experiments at JLC,” arXiv:hep-ph/0109166.
- [30] G. Weiglein *et al.* [LHC/LC Study Group], “Physics interplay of the LHC and the ILC,” arXiv:hep-ph/0410364.
- [31] J. A. Aguilar-Saavedra *et al.*, Eur. Phys. J. C **46**, 43 (2006) [arXiv:hep-ph/0511344].
- [32] P. N. Pandita and C. Sharma, Phys. Rev. D **85**, 015021 (2012) [arXiv:1112.6240 [hep-ph]].
- [33] J. R. Ellis, J. M. Frere, J. S. Hagelin, G. L. Kane and S. T. Petcov, Phys. Lett. B **132**, 436 (1983); E. Reya, Phys. Lett. B **133**, 245 (1983); P. Chiappetta, J. Soffer, P. Taxil, F. M. Renard and P. Sorba, Nucl. Phys. B **262**, 495 (1985), [Erratum-ibid. B **279**, 824 (1987)].
- [34] P. Fayet, Phys. Lett. B **117**, 460 (1982).
- [35] J. R. Ellis and J. S. Hagelin, Phys. Lett. B **122**, 303 (1983).
- [36] K. Grassie and P. N. Pandita, Phys. Rev. D **30**, 22 (1984).
- [37] T. Kobayashi and M. Kuroda, Phys. Lett. B **139**, 208 (1984).
- [38] J. D. Ware and M. E. Machacek, Phys. Lett. B **142**, 300 (1984).
- [39] L. Bento, J. C. Romao and A. Barroso, Phys. Rev. D **33**, 1488 (1986).
- [40] M. Chen, C. Dionisi, M. Martinez and X. Tata, Phys. Rept. **159**, 201 (1988).
- [41] T. Kon, Prog. Theor. Phys. **79**, 1006 (1988).
- [42] S. Y. Choi, J. S. Shim, H. S. Song, J. Song and C. Yu, Phys. Rev. D **60**, 013007 (1999) [arXiv:hep-ph/9901368].
- [43] A. Datta, A. Datta and S. Raychaudhuri, Eur. Phys. J. C **1**, 375 (1998) [arXiv:hep-ph/9605432]; A. Datta, A. Datta and S. Raychaudhuri, Phys. Lett. B **349**, 113 (1995) [arXiv:hep-ph/9411435].
- [44] S. Ambrosanio, B. Mele, G. Montagna, O. Nicrosini and F. Piccinini, Nucl. Phys. B **478**, 46 (1996) [arXiv:hep-ph/9601292].
- [45] A. Heister *et al.* [ALEPH Collaboration], Eur. Phys. J. C **28**, 1 (2003).
- [46] J. Abdallah *et al.* [DELPHI Collaboration], Eur. Phys. J. C **38**, 395 (2005) [arXiv:hep-ex/0406019].
- [47] P. Achard *et al.* [L3 Collaboration], Phys. Lett. B **587**, 16 (2004) [arXiv:hep-ex/0402002].
- [48] G. Abbiendi *et al.* [OPAL Collaboration], Eur. Phys. J. C **29**, 479 (2003) [arXiv:hep-ex/0210043].
- [49] G. Abbiendi *et al.* [OPAL Collaboration], Eur. Phys. J. C **18**, 253 (2000) [arXiv:hep-ex/0005002].
- [50] K. J. F. Gaemers, R. Gastmans and F. M. Renard, Phys. Rev. D **19**, 1605 (1979).

- [51] H. E. Haber and G. L. Kane, Phys. Rept. **117**, 75 (1985).
- [52] LEPSUSYWG, ALEPH, DELPHI, L3 and OPAL experiments, note LEPSUSYWG/01-03.1 (<http://lepsusy.web.cern.ch/lepsusy/Welcome.html>).
- [53] W. M. Yao *et al.* [Particle Data Group], J. Phys. G **33**, 1 (2006).
- [54] J. Abdallah *et al.* [DELPHI Collaboration], Eur. Phys. J. C **31**, 421 (2004) [arXiv:hep-ex/0311019].
- [55] H. K. Dreiner, S. Heinemeyer, O. Kittel, U. Langenfeld, A. M. Weber and G. Weiglein, arXiv:0901.3485 [hep-ph].
- [56] A. Pukhov, arXiv:hep-ph/0412191.
- [57] P. Ramond, arXiv:hep-ph/9809459.
- [58] S. P. Martin and P. Ramond, Phys. Rev. D **48**, 5365 (1993) [arXiv:hep-ph/9306314].
- [59] S. P. Martin, Phys. Rev. D **79**, 095019 (2009) [arXiv:0903.3568 [hep-ph]].
- [60] S. Eidelman *et al.* [Particle Data Group], Phys. Lett. B **592**, 1 (2004).
- [61] E.A. Kuraev, V.S. Fadin, Sov. J. Nucl. Phys. **41**, 466 (1985) [Yad. Fiz. **41**, 733 (1985)]
- [62] O. Nicrosini, L. Trentadue, Phys. Lett. B **196**, 551 (1987)
- [63] M. Skrzypek and S. Jadach, Z. Phys. C **49**, 577 (1991).
- [64] R. Blankenbecler and S. D. Drell, Phys. Rev. D **36**, 277 (1987).
- [65] J. Brau, (ed.), Y. Okada, (ed.), N. J. Walker, (ed.), A. Djouadi, (ed.), J. Lykken, (ed.), K. Monig, (ed.), M. Oreglia, (ed.) and S. Yamashita, (ed.) *et al.*, ILC-REPORT-2007-001.
- [66] H. K. Dreiner, O. Kittel and U. Langenfeld, Phys. Rev. D **74**, 115010 (2006) [arXiv:hep-ph/0610020].
- [67] A. Djouadi, J. -L. Kneur and G. Moultaka, Comput. Phys. Commun. **176**, 426 (2007) [hep-ph/0211331].
- [68] C. H. Chen, M. Drees and J. F. Gunion, Phys. Rev. Lett. **76**, 2002 (1996) [hep-ph/9512230].
- [69] F. A. Berends, G. J. H. Burgers, C. Mana, M. Martinez and W. L. van Neerven, Nucl. Phys. B **301**, 583 (1988).
- [70] F. Boudjema *et al.*, arXiv:hep-ph/9601224.
- [71] G. Montagna, M. Moretti, O. Nicrosini and F. Piccinini, Nucl. Phys. B **541**, 31 (1999) [arXiv:hep-ph/9807465].
- [72] F. Franke and H. Fraas, Phys. Rev. D **49**, 3126 (1994).
- [73] H. E. Haber and D. Wyler, Nucl. Phys. B **323**, 267 (1989).
- [74] S. Ambrosanio and B. Mele, Phys. Rev. D **53**, 2541 (1996) [arXiv:hep-ph/9508237].
- [75] S. Ambrosanio and B. Mele, Phys. Rev. D **55**, 1399 (1997) [Erratum-ibid. D **56**, 3157 (1997)] [arXiv:hep-ph/9609212].
- [76] H. Baer and T. Krupovnickas, JHEP **0209**, 038 (2002) [arXiv:hep-ph/0208277].
- [77] P.N. Pandita, Monalisa Patra, in preparation.
- [78] ATLAS Collaboration, *Search for squarks and gluinos using final states with jets and missing transverse momentum with the ATLAS detector in $\sqrt{s} = 7$ TeV proton- proton collisions*, ATLAS-CONF-2012-033 (2012).
- [79] CMS Collaboration, *Search for supersymmetry with the razor variables*, CMS-PAS-SUS-12-005 (2012)
- [80] CMS Collaboration, *Search for New Physics in Events with Same-sign Dileptons, b-tagged Jets and Missing Energy*, CMS-PAS-SUS-11-020 (2011).